Utrecht, 23 June 2016

Ref: acpd-15-21219-2015_revision2

Dear Editor,

On behalf of the co-authors of the article acpd-15-21219-2015 (Albert et al.: Parameterization of oceanic whitecap fraction based on satellite observations) I have uploaded the second revision of the manuscript, as well as the response to the reviewer.

We have substantially revised the manuscript, addressing each comment of the reviewer and following up on suggestions and criticism. We have also revised and/or added figures and tables. Point-by-point response to reviewer's comments is also given together with marked-up changes to track the revisions. With all this, we feel that the manuscript has been much improved.

Sincerely yours,

Monique Albert, on behalf of all co-authors.

Review of “Parameterization of oceanic whitecap fraction based on satellite observations” by Albert et al.

I was asked by the editor Michael Schulz to give feedback on this revised version. Below, I give my opinion on how selected comments from the initial two reviewers were addressed. This is followed by a conventional review of the revised manuscript.

We thank the reviewer for the time and effort in reviewing both our responses and the revised manuscript. Below are our responses to reviewer’s comments on selected comments from the initial two reviewers. Reviewer’s recurring comments are on two main points:

(1) Use of n = 2 instead of free parameter n; and

(2) Extended analysis of the effects of the wave field.

Our point-by-point responses below clarify that:

(1) Parameter n was first determined as a free parameter and found to be not statistically different from n = 2, thus n = 2 was used in the analysis;

(2) We use an early version of the whitecap database in which we have data for whitecap fraction at 10 and 37 GHz, wind speed, wind direction, and SST (W10, W37, U10, Udir, SST). With this early version of the whitecap database, we have investigated the effect of SST on the W variability and addressed the effect of wind field using proxy analysis of increasing/decreasing winds. The results on both effects were reported in both the initial and revised manuscripts.

In addition to these responses, we give the revised manuscript with track changes (text in blue is old text moved to a new place; text in red is new added text).

Point-by-point responses follow below.

Reviewer 1.

1.1) "Poor flow to manuscript" – Manuscript flow in section 3 still needs to be improved.

Section 3 is revised for clarity.

1.2) "Authors fail to distinguish the proposed formulation from SAL13" – I believe this point is still valid.

The first revision of the manuscript highlighted how the new parameterization differs from that of SAL13 (and other parameterizations) in two places:

Old p. 28, lines 17-19: "..when we model both the trend and the spread of the W values, the result is a significant difference with any, new or old, W(U10) parameterization at any conditions."

Old p. 33, lines 3-5: "The capability of the new W(U10, T) parameterization to model both the trend and the spread of the W data sets it apart from all other W(U10) parameterizations."

To address the reviewer's comment, the text is revised to read:

new p. 32 lines 25-27: "The capability of the new W(U10, T) parameterization to model both the trend and the spread of the W data sets it apart from all other W(U10) parameterizations (e.g., MOM80 and SAL13)."

new p. 32-33, lines 30-2: "While SAL13 analysis of the satellite-based whitecap database demonstrated the influences of secondary factors on whitecap fraction, our study goes a step further in using the satellite-based W data to parameterize one of these influences, that of SST."

1.3) "Discussion regarding 37GHz vs 10GHz intercept is not convincing" – This is now better in the revised manuscript. But, I do not agree that too much physical insight can be inferred about the sign and trend of the y-intercept (for the 37GHz data) without first letting the wind speed exponent be a free parameter (or showing it is not statistically different to 2).

We have done what the reviewer suggests here—we have used Eq. (6) with n as a free parameter; the results showed n values close to 2. Because we need unified expression for the globally-averaged trend to be applied to regional and seasonal subsets of W data, we settled on n = 2.

We conveyed this on old p. 19 (line 16-17) by saying: "Following the arguments of our approach (Sect. 2.1) and trying different expressions, we found that a quadratic wind speed exponent (n = 2) fits both W10 and W37 data sets best."

To address the reviewer's comment, we extended the text on this. Please see:

a) New p. 9 (lines 3-14)—text why we need mean wind speed trend to interpret the variations of regression coefficients a and b.

b) First paragraph of sect. 2.3 (new p. 14-15 lines 21-3) with new Table 2 where we show that the n values determined as free parameter are not statistically different from 2.

1.4) "Discussion about the "secondary factors" being "imbedded in the exponent of the wind speed dependencies" is misleading." – While I may not have used the term "misleading", I generally agree with the reviewer on this point. In their rebuttal Albert et al. state that "Anguelova and Webster (2006) …. suggest that the influence of secondary factors is expressed as a change of the wind speed exponent", yet here the authors have chosen to fix their wind speed exponent to 2.

As said in the response above—we determined n first as a free parameters and fixed it for the regional analysis in order to fix the mean trend and isolate regional fluctuations in coefficients a and b. The free parameters n for W10 and W37 data which we found (new Table 2) are not statistically different from 2. Thus using n = 2 is in a sense adjusted wind speed exponent which is also suitable for consistent regional analysis.

Additionally, I found the discussion of the statistical significance of SST effects confusing.

Sections 3.2 and 3.3 are now revised for clarity.

Furthermore, the authors refer to SAL13 and state on page 32 line 3-5 that wave field development is the most important secondary factor accounting for variability in W after wind speed, yet this was not investigated here.

The whitecap database used here includes data for W10, W37, U10, Udir, SST. This is the first version of the whitecap database. It differs from the extended version of the whitecap database, which SAL13 used, by including air temperature and wave field characteristics (significant wave height and peak wave period) matched in time and space with the W data. We describe the W database with which we work in section 2.2.1. On old p. 11, line 16-17, we said "In this study, we used daily match-ups of W, U10, and T data for each grid cell for the year 2006." We never mention in this section that the whitecap database contains data for the wave characteristics.

The analysis presented here does what is possible with this early version of the whitecap database. With these data, we did investigate possible effect of the wind field using as a proxy analysis of increasing and decreasing wind, as did Stramska and Petelski (2003) and Godijn-Murphy et al. (2011). Because the results on this analysis were limited, we reported them with one paragraph on old p. 21, lines 6-20.

To address the reviewer's comment, we revised the text as follows:

1) On the early version of the whitecap database, please see new pages: p. 3 lines 15-23; p. 6 lines 24-26; p. 11-12 lines 31-2.

2) On the wave field effect on W, please see:

a) The last paragraph in Sect. 2.3—new p. 16 lines 15-31;

b) The updated paragraph in Sect. 3.1.1—new p. 22-23 lines 23-3;

c) The sentence in Sect. 4 (Conclusions)—new p. 32, lines 13-15.

Therefore without presented evidence to the contrary, it is possible that any inferences regarding the influence of SST may be inadvertently due to wave field variability.

We agree with this statement and acknowledge that we did not clarify this point well in the first revisions of the text. To address the reviewer's comment, we do the following:

1) Clarify in Sect. 2.1 that the regional variations are due to all secondary factors (new p. 9 lines 3-14).

2) Note in Sect. 3.2.2 that it is not practical to use our limited results on the wave field effect to quantify regional variations of regression coefficients a and b (new p. 25 lines 23-31 and p. 26 lines 1-5).

Reviewer 2.

2.1) "Results and conclusions are rather limited. The paper has potential, but needs additional work." – In my opinion this comment still stands. I am not convinced that the authors have gone above and beyond what was presented in SAL13. I do not see the utility of another parameterization for the same W dataset presented in SAL13.

Generally, we believe that the W database (as any other datasets) can be used for different analyses by different groups with different or complementary results. This is the spirit behind sharing data among colleagues.

Specifically, the development of satellite-based W data was pursued with the idea to derive W parameterizations including many additional parameters (Anguelova and Webster, 2006). Here, using the early version of the W database, we present use of the satellite-based W data toward this goal by developing W(U10, T) parameterization. In this sense, the work we present is certainly a step further from previous analyses such as that of SAL13.

The utility of the new W(U10,T) parameterization is that it is able to predict the spread of the satellite-based W data. We showed this in the first revision of the manuscript in Fig. 13a and discussed this in old Sect. 3.3.2. SAL13 used the extended W database to show the variability of W as a function of different variables. And SAL13 made the first important parameterization W(U10) with this database. Note, however, that any W(U10) expression predicts the trend of the W with wind speed, but W(U10) expressions do not predict the spread of the data caused by other factors.

To address the reviewer's comment, we revised the manuscript to clearly convey the following points:

1) The new W(U10,T) parameterization is able to predict both trend and spread of the satellite-based W data and this sets it apart from other parameterizations: new p. 28 lines 15-20 with updated Fig. 13a; new p. 32 lines 25-27.

3) Directly state the difference between this study and SAL13 study: new p. 32-33 lines 30-2.

A more fruitful line of enquiry may be to apply the results of SAL13 to SSA emission flux predictions

This has been done—SAL13 parameterization has been used to estimate sea spray production and CO2 transfer velocity. It was presented at the 7th Gas transfer at water surface symposium

and a peer-reviewed proceeding paper is now published (Anguelova, IOP Conf. Ser.: Earth Environ. Sci. 35, 012002 2016).

To address the reviewer's comment, we cite Anguelova (2016) in Sect. 2.4: new p. 17 lines 8-10.

and/or present a more thorough comparison of regional differences in W variability by considering wave and temperature effects.

Again (see response above)—with the early version of the whitecap database that we use, we have addressed both SST effect and the wave field effect; proxy analysis of increasing/decreasing winds was used for the wave field effect. In the first revision of the manuscript, we have reported extensively the results on SST effect (Sect. 3.2) and gave a summary of the limited results on the wave effect in Sect. 3.1 (old p. 21, lines 6-20).

To address the reviewer's comment, once again we summarize the revisions we did regarding SST and wave field:

1) We added a new paragraph in Sect. 2.3 regarding the proxy analysis of the wave field effect.

2) We extended the discussion on SST in Sect. 3.2.2 with a new paragraph to clearly show our rationale for not quantifying the regional variations of coefficients a and b an terms of wave field.

2.2) "Regardless of the well correlated linear fits of sqrt(W) there is little justification why it should be quadratic" - I agree with the reviewer, and this aspect has not been sufficiently supported or defended in the actual manuscript. The inclusion of an investigation of a cubic wind speed dependence in the paper serves little purpose.

The emergence of quadratic wind speed exponent is already discussed above. To reiterate—we have determined n first as a free parameter and found it to be not significantly different from n=2, which is a suitable choice for consistent regional analysis.

In our view, the investigation of the cubic relationship is useful because it shows that when looking for the wind trend, it is better to base it on the available data than on purely theoretical basis. Using the available data in the whitecap database, the wind trend is close to quadratic and the use of n=2 is in essence empirically adjusted wind speed exponent.

To address the reviewer's comment, we revise the text to minimize the description of the analysis on cubic relationship, yet retain the basic results which we find useful. The investigation on the cubic wind speed dependence is now presented as follows:

1) One paragraph in Sect. 2.3: new p. 16 lines 1-14

2) One paragraph in Sect. 3.2.2: new p. 26 lines 16-22

3) One paragraph in Sect. 3.3.1: new p. 27-28 lines 22-2

4) One sentence In Sect. 4 (Conclusion): new p. 32 lines 28-30

2.3) "Progress over the extensively referenced Salisbury et al. paper is poorly documented or highlighted" – I still believe this is a valid comment.

This comment is the same as comment 2.1 above, so our response is the same: We make a step further in using satellite-based W data by employing the early version of the whitecap database to quantify SST effect on W. Please refer to our response to comment 2.1 for details.

2.4) "The main advantage of the paper might be exploration of regional differences" – I agree with the reviewer, and believe this should be the focus of a revised paper, with more thorough evaluation of combined wave field effects and SST effects.

Again, this point has been already addressed in the responses above—with the early version of the W database, we have done what can be done regarding the wave field effect. Our first revision of the manuscript had been extensively revised to expand the regional analysis. Our new revision includes one new paragraph to slightly extend the presentation of our proxy analysis of the wave field effect. Please refer to our response to comment 2.1 for details.

2.5) "I disagree with the concept of avoiding intrinsic correlation of W and U10 substituting QSCAT wind speed by ECMWF wind. In fairness, W should have been fitted directly to ECMWF data of whatever resolution because a large scatter (regardless of good overall correlation) between two wind speed datasets could have produced discernible differences in W." – From what I understand of the satellite retrieval algorithm, some intrinsic correlation is to be expected when W is parameterized with U10QSCAT. This is evident in the reduced scatter when W is plotted against U10QSCAT in comparison to U10ECMWF in the revised paper (figures 6 and 7). The authors have tried to evaluate this. However, in addition, I suggest that the difference in W data scatter when using U10QSCAT in comparison to U10ECMWF be quantified by evaluating W data spread at specific values of U10 for each wind speed source.

We implemented the calculations suggested above. Still, we decided to not include them in the second revision of the manuscript because these results give information similar to the one suggested in comment (iii) below. To address both comments (2.5 and iii), we computed rms deviation for each parameterization (Eq. (11) for QSCAT and Eq. (12) for ECMWF) in reference to the satellite-based W data. The results are shown in new Fig. 8 as residual plots and discussed in Sect. 3.1.2 (new p. 23 lines 23-28).

Ideally, for robustness, any statistical inferences between W variability and SST (or other forcing factors) could also be evaluated using both sources of wind speed data.

Yes, we agree with this statement.

However, once the discrepancies due to the use of different sources are described (Fig. 4 and Sect. 3.1.2), we use U10 and T from the whitecap database for all analyses and results in order to minimize uncertainties introduced by using different sources and different matching procedures. We gave our arguments for this decision in one paragraph in Sect. 2.3 in the first revision of the manuscript (old p. 14 lines 25-30 and p. 15 lines 1-3). The same decision and paragraph are retained in the second revision of the manuscript (new p. 15 lines 22-30).

However, it should not be forgotten that the retrieval of W using satellites represents a very important progression in remote sensing capabilities and will no doubt continue to improve. As long as the magnitude of intrinsic correlation is known, progress can still be made.

Yes, we agree with the last statement. For this reason we evaluated and reported the intrinsic correlation (section 3.1.2) and concluded on old p. 22, lines 23-24: "We, therefore, conclude that the effect of the intrinsic correlation alone on W is most likely less than about 4% for most wind speeds." This conclusion remains in Sect. 3.1.2 (new p. 24 lines 5-10).

Review

Overall evaluation.

The authors have clearly invested significant effort into this manuscript, and into the revisions. This effort is recognized by this reviewer.

We appreciate the time and efforts of the reviewer. We are also thankful that the reviewer acknowledges the extensive additional work done following the suggestions of two initial reviewers and the comment of Brooks and Salisbury.

Substantial revisions have been done for the second revision of the manuscript to address the reviewer's comments. Point-by-point responses follow below.

However, I find that that many of the initial concerns of the 2 reviewers to be still valid.

This comment is already addressed with our responses above.

For this reason, I suggest the paper needs further work or a change of focus. For example, the focus could be shifted to provide more detail on regional differences in W (perhaps using a more limited number of regions) to really derive more physical insight into W variability in relation to a wider range of factors other than SST, which can then be applied to SSA flux. Also, detailed spectral model wave data (e.g. from ECMWF wave model or similar) could be incorporated into a revised study to complement the existing data sources.

The work presented here has focused from the beginning on the utility of the early version of the whitecap database (consisting of W10, W37, U10, Udir, SST) in regard to parameterizing W and modifying the sea spray source function (SSSF). Therefore, with this whitecap database, we have addressed W(SST) variability, the wave field effect using proxy analysis, and sea spray production using the new W(U10, T) parameterization. We are confident that this research inquiry is necessary and worthy in two aspects: (1) In regard to using satellite-based W data to quantify W variability (SST in our case); and (2) In regard to current efforts in the air-sea in interaction community to introduce SST dependence (among others) in the sea spray source function. We document these efforts with the numerous references on SSSF in our initial and revised manuscripts.

Variability and parameterization of W with wave characteristics is certainly of interest and will be pursued as a future work. This topic can be addressed with the extended whitecap database, which we do not have. Extending this whitecap database with wave data and quantifying the wave field impact on W is, in effect, a full new project worthy of a PhD dissertation. Moreover, during the course of the study we present, Anguelova and co-workers continued to work on compiling the extended database and we did not see a reason to duplicate their effort.

Importantly, Anguelova and co-workers provide match-ups of W and other variables in the fine swath resolution of WindSat, before gridding all variables for the whitecap database. Any matchups made with modeled data (e.g., from ECMWF) in gridded format are too crude and introduce more spread to the W data. Our investigation on the intrinsic correlation shows this clearly.

Alternatively, the authors could follow on from the Salisbury et al. papers and apply the results already derived from that work to SSA flux, and potentially, to gas flux.

As already mentioned above—this has already been done (Anguelova, IOP Conf. Ser.: Earth Environ. Sci. 35, 012002 2016) and we cite Anguelova (2016). The effort described in our manuscript differ from that of Anguelova (2016) by applying the new W(U10, T) parameterization to evaluate SSA flux.

General Comments

i) The authors have not presented a convincing case that fixing the wind speed exponent to 2 in their parameterisations is justified. I believe that it should be a free parameter, as this will have implications for how they physically interpret the resulting fit coefficients. If, however, they show that the wind speed exponent is not significantly different to 2, (I.e. is within 95% confidence intervals of 2), then they would be more justified in their analysis, and this would be acceptable.

In the responses above we have addressed this comment (e.g., see response to comment 1.3).

To reiterate: we have used Eq. (6) with n as a free parameter; the results showed n values close to 2. Because we need unified expression for the globally-averaged trend to be applied to regional and seasonal subsets of W data, we settled on n = 2.

We conveyed this on old p. 19 (line 16-17) by saying: "Following the arguments of our approach (Sect. 2.1) and **trying different expressions**, we found that a quadratic wind speed exponent (n = 2) fits both W10 and W37 data sets best."

The reviewer's repeated comments on this point show that we didn't convey this information clearly.

The second revision of the manuscript addresses this point more specifically with the following:

a) Extended paragraph in Sect. 2.1 (new p. 9 lines 3-14) to clarify why we need mean wind speed trend to interpret the variations of regression coefficients a and b.

b) New Table 2 lists the n values determined as free parameter and new paragraph in Sect. 2.3 (new p. 14-15 lines 21-3) describing the analysis and showing that the free-parameters n are not statistically different from 2 within 95% confidence intervals.

ii) The authors state that wave field development is the second biggest factor influencing W, after U10, yet this was not considered at all in the study. Therefore, any conclusions related to SST are limited and may be due to potential correlations between SST and wave field development.

This comment was already addressed in several responses above. To reiterate:

1) The data set used in this study is an early version of the whitecap database which does not include characteristics of the wave field. So we proceed with what can be done with this data set, namely, develop W-SST relationship.

2) With the data available, we did address the influence of the wave field by considering the effect of increasing and decreasing wind (proxy for young and mature seas). Early versions of the manuscript included more information on this proxy analysis and showed weak influence of the wave field on W. Because the results were limited, we restricted the information on this proxy analysis to the paragraph given in old Sect. 3.1.1 (old p. 21, lines 6-20).

3) The reviewer mentions here "potential correlation between SST and wave field." This statement can be understood in different ways. If the reviewer meant influence of SST on the wave field growth, we note that this is an actively pursued topic within the air-sea interaction community and it is out of the scope of this work. Direct SST-waves relationship is not established. Usually the effect of SST fronts on wind stress via atmospheric stability is studied (e.g., O'Neill et al., 2012, J. Climate, DOI: 10.1175/JCLI-D-11-00230.1). Moreover, the direct effect of SST is mostly on the small scale roughness (e.g., Grodsky et al., 2012, GRL, doi:10.1029/2012GL052091) and it is most effective in strong SST gradients formed after hurricane passage (e.g., Chen et al., 2013, JAS, DOI: 10.1175/JAS-D-12-0157.1). None of these effects can be studied with the whitecap database used here which includes winds up to 35 m/s and does not include wave field characteristics. Even the extended whitecap database would not be suitable to study these topics/effects because the wave characteristics which it includes (significant wave height and peak wave period) cannot resolve the effect which SST imparts on small scale roughness.

We believe, however, that by "potential correlation between SST and wave field" the reviewer meant that when studying the regional variations, we cannot separate (deconvolve) the effects of SST and wave field on W data. We responded to this comment in our response to comment 1.4 above. We agree with this statement and acknowledge that we did not clarify this point well in the first revisions of the text. With such understanding, we did the following to address the reviewer's comment:

1) Clarify in Sect. 2.1 that the regional variations are due to all secondary factors (new p. 9 lines 3-14).

2) Note in Sect. 3.2.2 that it is not practical to use our limited results on the wave field effect to quantify regional variations of regression coefficients a and b (new p. 25 lines 23-31 and p. 26 lines 1-5).

iii) An additional quantification of potential self-correlation between W and U10QSCAT could be provided. For example, a measure of the data scatter around the W-U10ECMWF and W-U10QSCAT parameterizations, as a function of wind speed, could be presented. This could be done as an rms error as a function of wind speed for each wind speed product, and/or by showing

W residuals as a function of wind speed. I suggest this because of the quite large difference in the spread of W(U10) values in figure 7 when compared with figure 6b (i.e. using two estimates of U10). (Is it the same for 10GHz data?)

In the first revision of the manuscript, we have presented two metrics to detect and evaluate the intrinsic correlation: change of the correlation coefficients of the W–U10 relationships when different wind speed sources are used and percent difference between W values predicted by W(U10QSCAT) and W(U10ECMWF) expressions.

Following the suggestion in this comment (and a similar one given in comment 2.5 above), we include a new Fig. 8 to plot as a function of wind speed the residuals (biases) between satellite-based W data and predicted W values using U10QSCAT and U10ECMWF (Eq. (11) for QSCAT and Eq. (12) for ECMWF). We also report the rms deviations for each data set. The results are discussed in Sect. 3.1.2 (new p. 23 lines 23-28).

Performing subsequent statistical tests on W data variability in relation to secondary factors using U10QSCAT and U10ECMWF are likely to be different, and potentially significantly so.

For secondary factors, our Fig. 4b shows that SST values from different sources are in fact quite similar. This implies that using SST from different sources would not add to the W variability.

However, differences coming from the use of U10 values from different sources and the crude matching procedure introduce additional variability for all W–U10ECMWF data pairs. To avoid these additional discrepancies, once we quantify the relationship between U10QSCAT and U10ECMWF, we continue our analysis using U10QSCAT. We gave our arguments for this decision in one paragraph in Sect. 2.3 in the first revision of the manuscript (old p. 14 lines 25-30 and p. 15 lines 1-3). The same decision and paragraph are retained in the second revision of the manuscript (new p. 15 lines 24-30). We give the rationale for this decision with the paragraph on new p. 14 lines 15-19.

iv) Regarding the flow of the manuscript, I found the text to be improved but still confusing in several locations (especially in several parts of section 3) suggesting that significant points could be better articulated.

Revisions of the flow and clarity of the manuscript in section 3 have been done, namely:

1) Shorten the text on the cubic W(U10) relationship.

2) Shorten and clarify the description of Fig. 12

3) Focus discussion on regression coefficients a and b and retain only basic info on coefficients m and c.

The revisions can be tracked in the marked-up manuscript which follows these responses.

Specific notes

Page 2. Line 12. The mean whitecap coverage estimate from Blanchard is given as 1.2X10^17, which corresponds to about a 3.33% coverage.

Yes, agreed. Both the estimate given by the reviewer and the range we cited (2% to 5% in line 12 on p. 2) are from Table 3 in Blanchard (1963, p. 162). The range we gave reflects seasonal and geographical variations according to Blanchard (1963). To give strictly annual global average W, we revised the text to 3.4% (p. 2, line 10).

Figure 4(a,b) should be presented with logarithmic y-axis.

Figure 4 (a, b) gives 1:1 graphs for U10 and SST from different sources. Neither U10 nor SST needs to be presented on logarithmic scale.

We believe the reviewer had in mind Fig. 5 (a, b). This is now done: panels c and d are added with the same data as in panels a and b but in logarithmic y-axis. The text is revised accordingly (new p. 20 lines 2-4).

Page 8, line 13-14. Then why was n fixed to 2 here when investigating different regional variations?

This is a recurring question and comment to which we have responded several times. Please see response to comment (i) above.

Pag3 14, line 14. When all satellite W data are included, how does the data spread compare to the spread in in-situ W data? Does it cover the same 3 orders of magnitude variability?

Figure 1b with W data at 10 and 37 GHz for one day and Fig. 5 with all 2006 W data at a given frequency show that at a given (fixed) wind speed, the spread of the satellite-based W data is much smaller than the spread of the in situ data. For example, at wind speed of 10 m s^{-1}, Fig. 1b shows spread of the in situ data over 3 orders of magnitude, while Fig. 5a and b show spread of the satellite W data within one order of magnitude.

Page 16 Line 6. Why is the timescale absorbed into the shape factor?

Monahan et al. (1986) give (Eq. (4) in the manuscript):

$$\frac{dF}{dr_{80}} = \frac{W(U_{10})}{\tau}\frac{dE}{dr_{80}} = 1.373 \cdot U_{10}^{3.41} \cdot r_{80}^{-3}(1 + 0.057 r_{80}^{1.05}) \times 10^{1.19 e^{-B^2}}$$

Representing W(U10) of MOM80 separately gives:

$$\frac{dF}{dr_{80}} = \frac{W(U_{10})}{\tau}\frac{dE}{dr_{80}} = W(U_{10})\left[\frac{1}{\tau}\frac{dE}{dr_{80}}\right] = 3.84\times10^{-6}U_{10}^{3.41}\left[\frac{1}{\tau}\frac{dE}{dr_{80}}\right] =$$
$$= 3.84\times10^{-6}U_{10}^{3.41}\left[\frac{1.373}{3.84\times10^{-6}}r_{80}^{-3}(1+0.057r_{80}^{1.05})\times10^{1.19e^{-B^2}}\right]$$

This leads to

$$\frac{dF}{dr_{80}} = 3.84\times10^{-6}U_{10}^{3.41}\left[3.56\times10^{5}\,r_{80}^{-3}(1+0.057r_{80}^{1.05})\times10^{1.19e^{-B^2}}\right] =$$
$$= W(U_{10})\left[3.56\times10^{5}\,r_{80}^{-3}(1+0.057r_{80}^{1.05})\times10^{1.19e^{-B^2}}\right]$$

with timescale τ in coefficient 3.5755×10^{5}. We replace W(U10) with W(U10,T) to get Eq. (4′).

Figure 5. On lines 1-5, page 11, the authors state that W37 should always be greater than W10. Yet, Figure 5 suggests this is violated sometimes.

Yes, in most cases W37>W10 and Fig.1b shows this more clearly than Fig. 5. At high winds (e.g., U10 > 15 m/s), foam layers become increasingly thicker for both active and residual (decaying) foam. So W10 is increasingly representative of both whitecap lifetime stages. In this way W10 and W37 become increasing similar. In such conditions, there could be cases for which W37<W10.

We revised line 19 on new p. 11 to read "*W*37 data are usually larger than *W*10 data."

Pg19, Lines 1-2. Why is wave field development not addressed here given the statement further into the manuscript? (see page 32, line 3-5)

Lines 1-2 on old p. 19 read (new p. 20 lines 8-10) read: "suggestion that other variables, in addition to *U*10, influence the whitecap fraction, such as SST or wave field; SAL13 quantify this variability."

This text is in Sect. 3.1 where we give general observations about the satellite-based W data shown in Fig. 5. We draw the reader's attention to the fact that satellite-based W data carry information on secondary factors; we mention SST and wave field as examples for such secondary factors. Because SAL13 have already investigated the variability of W on these factors, we cite their paper.

The following subsection 3.1.1 quantified the average wind speed dependence as we need it for the regional analysis. In this section, we addressed the effect of the wave field on W by discussing our analysis of W against increasing and decreasing wind speed (proxy for young and mature seas); these were lines 6-20 on old p. 21. This paragraph is now revised (new p. 22 lines 23-32 and p. 23 lines 1-3). I addition, a new paragraph is added in Sect. 2.3 (new p. 16 lines 15-

31) to extend the representation of our proxy analysis for wave field via increasing/decreasing winds.

In the following subsections of Sect. 3, we quantify the SST dependence of W because the early version of the whitecap database, which we use, is suitable for such investigation. The W-SST analysis is useful step toward the goal of using the satellite-based W database to introduce additional variables in W parameterizations.

Lines 3-5 on page 32 in the end of the manuscript (after presenting all our results on W-SST analysis) were in effect a suggestion for further work. This phrase is now moved up in the text to introduce the new paragraph in the end of Sect. 2.3

Page 20, line 5. Wind speed product plays a role in the variability. For example, and as commented upon in SAL13, using the same W dataset but wind speed from QuikSCAT and ECMWF, Goddijn-Murphy et al (2011) found the exponent on a simple wind speed only whitecap coverage parameterization to change by a factor of 2 from 1.86 (±0.14) to 3.76 (±0.20). The only way to investigate if such an effect is seen in this study is to use a parameterization of the form W = a (U10 + b)^n, with both sources of wind, where all fitting coefficients are free parameters, and n is not pre-determined.

We agree with the reviewer that the source of the wind speed data contributes to the variability. In this manuscript, we have quantified this by giving the relationship between U10 from QuikSCAT and U10 from ECMWF in section 2.2.3, including Eq. (7) and Fig. 4a.

Our Eqs. (11) and (12) (sect. 3.1.2) are W(U10) parameterizations in the form W = a (U10 + b)^n using U10 from QuikSCAT and ECMWF, respectively. We use these equations to evaluate how much predictions of W would differ due to use of different wind speed sources.

Parameter n for both equations is n = 2 determined as described in the previous responses: first a specific n as a free parameter, which is found to be not statistically different from 2. Using the same n, the difference for the different sources is reflected in the regression coefficients of Eqs. (11) and (12). For example, coefficient b changes by a factor of 1.7 from 1.9 to 3.33.

Page 20 , lines 13-end, and Page 21, lines 1-5. While it is reasonable to assume that surfactants may stabilize foam so that it is present at wind speeds below 3 m/s, a discussion on the sign of the b coefficient in the formula (W = a (U10 + b)^n) must only be done after a fitting exercise which leaves the wind speed exponent (n) as a free-parameter.

Lines 13-end on old p. 20 and lines 1-5 on p. 21 promote a novel hypothesis that coefficient b with different signs can be considered as a mathematical expression of static forcing on W. We derive coefficients b for different regions when applying the same (mean) wind speed dependence. In this way, for each region we adjust the W(U10) to the same globally-averaged conditions and therefore are able to identify regional changes around this mean. In our view, exactly by fixing the wind speed dependence to the global mean conditions, we are able to

interpret the regional variations (or deviations) of b around this mean as caused by the regional characteristics.

Figure 7. The solid line in Figure 7 should go through the origin as reported in the legend. Figure7 could be presented with part a and b. Part a as is already presented, with part b on a logarithmic y-axis and with W in place of W^1/2.

The free and zero-forced fits in Fig. 7 are fixed, thank you.

Panel b for Fig. 7 now added to show W37 vs U10ECMWF with logarithmic y-axis to be compared to its counterpart in new Fig. 5d. The text is revised accordingly (new p. 23, lines 12-15).

Figure 8. The information presented in this figure may be better represented in a table where regions, seasons, and fit coefficients (along with 95% confidence intervals) are presented. As it stands, the information in figure 8 is poorly communicated to the reader.

Old Fig. 8 (new Fig. 9) conveys a lot of information in a compact way. Our tables with data for several variables (two regression coefficients, wind speed, and SST) for 12 months for 12 regions for 2 frequencies are long and would take 2-3 pages to publish. The values of the fit coefficients are quite similar (old Fig. 9 gave an idea for the values). The best way to grasp all this information is to show the behavior of the data, not the specific values. This is what old Fig. 8 (new Fig. 9) accomplishes: it combines the regression coefficients to represent $W^{1/2}$ and its variations with U10 between regions, months, and frequencies in a compact way that allows comparison among all these parameters.

To address the reviewer's suggestion, we added new Table 3 which lists values of slope (coefficient m), intercept (coefficient c), mean wind speed U10, mean SST, and the number of data points per region for March 2006 for all 12 regions for 10 and 37 GHz data. The text is revised accordingly in Sect. 3.2.1 (new p. 24 lines 19-21).

95% confidence intervals are needed on the datapoints presented in figure 9 (and on all fitting coefficients). Also, here and page 23 lines 21-29, stick to either evaluating potential trends in coefficients and or coefficients and . Otherwise it becomes too confusing for the reader.

With a few necessary exceptions, we now focus the discussion on coefficients a and b; we remove some text on coefficients m and c. In the same vein, we remove old Fig. 9.

Page 26, Line 24-26. Here, the authors are extrapolating the MOM function to wind speeds well beyond the range over which the MOM function was determined. This needs to be stated. Also, given the statement later on page 29 lines11-15, is this exercise valid?

We have stated that MOM80 is usually employed beyond its range of validity on old p. 4, lines 11-13 and old p. 29 lines 8-9. These statements remain in the second revision of the manuscript: new p. 4 lines 12-14; new p. 29 lines 5-8.

On old p. 26 (lines 24-26), we have applied MOM80 to all available wind speed values U10SCAT because using MOM80 (or any other SSSF) globally is a common practice (e.g., de Leeuw et al., 2011, their Fig. 1). To address the reviewer's comment, we revised Sect. 3.3.1 to discuss the comparison of parameterizations for the wind speed range of 3-20 m/s for which our parameterization W(U10,T) was developed.

For the statement on old p. 29 (lines 11-15): This sentence is now moved up at the start of Sect. 3 (new p. 19 lines 26-28). The purpose of this sentence is to point out the limitations of our results. Note, however, that the use of our new parameterization beyond 20 m/s is still a valid exercise because there are satellite-based W data beyond 20 m/s which can show how good or bad the extrapolation is. We have restricted the range over which W(U10,T) was developed only as a measure of quality control of the data, not because data are lacking (see new p. 15 lines 14-16).

Page 27, Lines 8-15. I don't understand this paragraph. The authors say that SST does not have a statistically significant effect on W values in the previous paragraph. Yet here, they say that a single quadratic parameterization, without additional temperature information, implicitly accounts for "most of the SST (and other) influences". But, how can they account for SST influences if they are not statistically significant, and how can they deconvolve this signal from other potentially stronger signals such as sea state development which has already been shown to be important in SAL13?

This paragraph and the entire Sect. 3.3.1 are now revised for clarity (new p. 27-28).

Briefly, the small variations with SST that we observe and find to be not significantly different from other parameterizations is due to partial accounting of the SST effect together with the effect of all other factors via the adjustment of the wind exponent to n = 2. The satellite-based W data carry information for the effect of U10 and all other factors. With the data we use, we cannot separate/deconvolve the effects of different factors. That is why we apply the globally average wind speed dependence (found to be n = 2) to all regions. In this way, we fix the mean trend and quantify the remaining fluctuations in different regions as a function of SST. However, this adjustment with n = 2 in effect already accounts for SST to some extent (as for all other effects) implicitly. With other words, we account on average for all factors (including SST) through n = 2 and we parameterize the remaining fluctuations through coefficients a(T) and b(T).

Page 27, Lines 16-24. It is my opinion that the wind speed exponent be a free-parameter.

The wind speed exponent was determined first as a free parameter. It was found to be not significantly different from 2 ($p > 0.05$), thus we use n = 2 for a consistent regional analysis.

Page 28, Line6-8. But the parameterization was generated using this dataset. So why is this a noteworthy result?

The noteworthy result is that the new W(U10,T) parameterization is able to model both the trend and the spread of the satellite-based W data. This is in contrast to previous W(U10) parameterizations which model only the trend of W with U10. The method of Anguelova and Webster (2006) to obtain satellite-based W data was developed with the idea to be able to model the natural variability (spread) of W.

Fig. 13a in the first revision of the manuscript used the same W data from 2006 to show that the new W(U10) and W(U10,T) parameterizations **replicate** the satellite-based data well. That is, even if one does not have satellite-based W data, the new W(U10) and W(U10,T) parameterizations can be used to calculate W values similar to those from satellite observations.

To address the reviewer's comment, Fig. 13a is updated to show the comparisons of the new W(U10) and W(U10,T) parameterizations to satellite-based data from 2007, values independent from those in 2006 used to derive the parameterizations. As the updated Fig. 13a shows, the results are the same as observed in Fig. 13a in the first revision of the manuscript.

The parameterization would likely follow the data even better if the exponent was a free parameter, and not fixed at 2.

Agree—it would be a better fit because it adjusts three parameters instead of two. However, the goal to fix the wind speed dependence is to have the global mean conditions as a reference against which to evaluate the regional variations due to regional factors.

Page 28, Line8-10. I believe this shows that secondary factors do not have a large influence on this satellite derived dataset.

The influence of the secondary factors on the satellite-based W data is such that the winds speed dependence is changed to be close to quadratic. After adjusting the wind speed dependence to $n < 3$ and thus accounting implicitly for the secondary factors, we quantify the **remaining** variations explicitly with a(T) and b(T). Taken together, the set of parametric coefficients—n = 2, a(T), and b(T)—accounts for the full SST effect. These clarifications are given in the second revision of the manuscript on new p. 9 lines 3-14 and new p. 27 lines 14-21.

Page28, Lines11-19. Here the authors have lost me. This is especially unfortunate since they state that this paragraph contains the most significant result of the paper. Also, (lines 16-17 specifically), SAL13 comment that satellite retrievals above 20 m/s be handled with caution, where W10 and W37 cross-over, which is not physically reasonable. I suggest that comments relating to differences in W parameterizations at wind speeds > 20 m/s be removed.

The paragraph on old p. 28 lines 11-19 is now revised for clarity (new p. 28 lines 10-20), including the reviewer's suggestion.

Page 28, Lines 25-31. The authors have not convinced me that any inferences on different combinations of U10 and T have systematic influences on W. Also, SAL13 have already derived parameterisations that are different from previous cubic parameterisations such as CAL08 and MOM80.

The discussion of Fig. 12 is now revised for clarity. Our Fig. 13a shows that accounting for at least one secondary factor, we are able to model some of the spread of the W data.

Yes, the SAL13 parameterization accounts well for the trend of the W data, still it does not account for the spread of the satellite-based W data. In this sense, the derived W(U10,T) parameterization adds to the skill of the W(U10) parameterization of SAL13. Though the explicit SST effect shown here is relatively small, our results point that adding SST and other secondary factors in future is the way to go if we are to improve predictions on regional scales beyond the mean conditions.

Page 29, lines 21-23. I am confused. The authors state on page 26, lines 20-24, that "ANOVA and Student tests show no significant difference" between the quadratic parameterization, and MOM80.

The statement on old p. 26, lines 20-24 was for parameterized W values in old Fig. 12a obtained with U10 =3-20 m/s (stated on old p. 26, line 11) for specific values of T.

The statement on old p. 29, lines 21-23 is related to the results in Fig. 13a, where the new W(U10,T) expression was used with U10 and T values from the whitecap database (stated on old p. 28 lines 1-3). The use of real data with W(U10,T) predicts a cluster of W values which are significantly different from those obtained with MOM80.

The discussion is now revised for clarity; please see Sect.3.3.1 (new p. 27-28) and Sect. 3.3.2 (new p. 28-29).

Page 32, line 3-5. If wave field development is more important than SST, then how can we evaluate any of the statements on SSA emission and W related to SST, when this has not been addressed in this manuscript?

The statement on old p 32, line 3-5, was in effect recommendation for future work. In this manuscript we addressed effects that we could with the early version of the whitecap database, namely SST. We also addressed the wave effect with a proxy analysis and found the results limited. To address the reviewer's comment, we revise this statement for clarity (new p. 33 lines 16-22).

Below follows the marked-up form of the revised manuscript.

The major revisions done are:

1) Extended text and new Table 2 to demonstrate that the wind speed exponents n obtained as free parameters are not statistically different from 2 within 95% confidence interval.

2) Extended text in Sect. 2.3 to more fully present our proxy analysis of the wave field effect using increasing/decreasing wind speeds.

4) New Figs. 7 and 8 and revised Sect. 3.1.2 to include reviewer's suggestions on evaluating the intrinsic correlation.

5) New Table 3 and updated Figs 5, 12, 13a

6) Extensive revision of Sects. 3.2 and 3.3 for flow and clarity.

Parameterization of oceanic whitecap fraction based on satellite observations

M. F. M. A. Albert[1], M. D. Anguelova[2], A. M. M. Manders[1], M. Schaap[1], and G. de Leeuw[1,3,4]

[1]{TNO, P.O. Box 80015, 3508 TA Utrecht, The Netherlands}

[2]{Remote Sensing Division, Naval Research Laboratory, Washington, DC 20375}

[3]{Climate Research Unit, Finnish Meteorological Institute, Helsinki, Finland}

[4]{Department of Physics, University of Helsinki, Helsinki, Finland}

Correspondence to: M. F. M. A. Albert (monique.albert@tno.nl)

Abstract

In this study the utility of satellite-based whitecap fraction (W) data for the prediction of sea spray aerosol (SSA) emission rates is explored. More specifically, the study aims at evaluating how an account for natural variability of whitecaps in the W parameterization would affect SSA mass flux predictions when using a sea spray source function (SSSF) based on the discrete whitecap method. The starting point is a data set containing W data for 2006 together with matching wind speed U_{10} and sea surface temperature (SST) T. Whitecap fraction W was estimated from observations of the ocean surface brightness temperature T_B by satellite-borne radiometers at two frequencies (10 and 37 GHz). A global scale assessment of the data set yielded a quadratic correlation between W and U_{10}. A new global $W(U_{10})$ parameterization was developed and used to evaluate an intrinsic correlation between W and U_{10} that could have been introduced while estimating W from T_B. A regional scale analysis over different seasons indicated significant differences of the coefficients of regional $W(U_{10})$ relationships. The effect of SST on W is explicitly accounted for in a new $W(U_{10}, T)$ parameterization. The analysis of W values obtained with the new $W(U_{10})$ and $W(U_{10}, T)$ parameterizations indicates that the influence of secondary factors on W is for the largest part embedded in the exponent of the wind speed dependence. In addition, the $W(U_{10}, T)$

Deleted: is

Deleted: ed

Deleted: ,

Deleted: , and statistical data

Deleted: revealed

parameterization is capable to partially model the spread (or variability) of the satellite-based W data. The satellite-based parameterization $W(U_{10}, T)$ was applied in an SSSF to estimate the global SSA emission rate. The thus obtained SSA production rate for 2006 of 4.4×10^{12} kg yr^{-1} is within previously reported estimates, however with distinctly different spatial distribution.

1 Introduction

Whitecaps are the surface phenomenon of bubbles near the ocean surface. They form at wind speeds of around 3 m s^{-1} and higher, when waves break and entrain air in the water which subsequently breaks up into bubbles which rise to the surface (Thorpe, 1982; Monahan and Ó'Muircheartaigh, 1986). The estimated annual global average of whitecap cover, i.e., the fraction of the ocean surface covered with whitecaps W, is 3.4% (Blanchard, 1963). Being visibly distinguishable from the rough sea surface, whitecaps are the most direct way to parameterize the enhancement of many air-sea exchange processes including gas- and heat transfer (Andreas, 1992; Fairall et al., 1994; Woolf, 1997; Wanninkhof et al., 2009), wave energy dissipation (Melville, 1996; Hanson and Phillips, 1999), and the production rate of sea spray aerosols (SSA) (e.g., Blanchard, 1963; 1983; Monahan et al., 1983; O'Dowd and de Leeuw, 2007, de Leeuw et al., 2011), because all these processes involve wave breaking and bubbles.

Deleted: 2 to 5

Measurements of the whitecap fraction W are usually extracted from photographs and video images collected from ships, towers, and air planes (Monahan, 1971; Asher and Wanninkhof, 1998; Callaghan and White, 2009; Kleiss and Melville, 2011). Whitecap fraction is commonly parameterized in terms of wind speed at a reference height of 10 m, U_{10}. Wind speed is the primary driving force for the formation and variability of W (Monahan and Ó'Muircheartaigh, 1986; Salisbury et al., 2013, hereafter SAL13). Whitecap fractions predicted with conventional $W(U_{10})$ parameterizations show a large spread between reported W values (Lewis and Schwartz, 2004; Anguelova and Webster, 2006). Part of these variations is due to differences in methods of extracting W from still and video images. Indeed, the spread of W data has decreased in recently published in situ data sets as image processing improved and data volume increased (de Leeuw et al., 2011). However, an order-of-magnitude scatter (spread) of W data remains, suggesting that U_{10} alone cannot fully predict the W variability. Other factors such as atmospheric stability (often expressed in terms of air-

sea temperature difference), sea surface temperature (SST) or friction velocity (combining wind speed and thermal stability (e.g., Wu, 1988; Stramska and Petelski, 2003)) have been indicated to affect W with implications for the SSA production. Thus, parameterizations of W that use different, or include additional (secondary), forcing parameters to better model the spread of W data due to natural whitecap variability have been sought (Monahan and Ó'Muircheartaigh, 1986; Zhao and Toba, 2001; Goddijn-Murphy et al., 2011; Norris et al., 2013b; Ovadnevaite et al., 2014; Savelyev et al., 2014).

Deleted: T

Deleted: account for

An alternative approach to address the variability of W is to use whitecap fraction estimates from satellite-based observations of the sea state, because such observations provide long-term global data sets which encompass a wide range of meteorological and environmental conditions, as opposed to local measurement campaigns during which a limited variation of conditions is usually encountered. Brightness temperature T_B of the ocean surface measured from satellite-based radiometers at microwave frequencies has been successfully used to retrieve geophysical variables, including wind speed (Wentz, 1997; Bettenhausen et al., 2006; Meissner and Wentz, 2012). The feasibility of estimating W from T_B has also been demonstrated (Wentz, 1983; Pandey and Kakar, 1982; Anguelova and Webster, 2006).

Anguelova et al. (2006; 2009) used WindSat data (Gaiser et al., 2004) to further develop the method of estimating W from T_B, and compiled a database of satellite-based W data accompanied with additional variables (hereafter referred to as whitecap database). An early version of the whitecap database combines whitecap fraction at two frequencies (W_{10} for 10 GHz and W_{37} for 37 GHz), with wind speed U_{10}, wind direction U_{dir}, and SST T. Figure 1a shows an example of the global W distribution from WindSat for a randomly chosen day from this whitecap database. An extended version of the whitecap database was compiled later to include three additional environmental variables: air temperature, significant wave height, and peak wave period (Anguelova et al., 2010).

Salisbury et al. (2013) analyzed the extended whitecap database and showed that satellite-based W values carry a wealth of information on the variability of W. In particular, these authors showed that the global distribution of satellite-based W values differs from that obtained using a conventional $W(U_{10})$ parameterization with important implications for modeling SSA production rate in global climate models (GCMs) and chemical transport models (CTMs) (Salisbury et al., 2014). Salisbury et al. (2013) proposed a new $W(U_{10})$ parameterization in power law form using satellite-based W data over the entire globe for a

full year. They derived wind speed exponents which are approximately quadratic for different data sets:

$$W_{10} = 4.6\times10^{-3}\times U_{10}^{2.26}; \qquad 2 < U_{10} \le 20 \text{ m s}^{-1},$$
$$W_{37} = 3.97\times10^{-2}\times U_{10}^{1.59}; \qquad 2 < U_{10} \le 20 \text{ m s}^{-1}, \tag{1}$$

where W is expressed in %. These exponents are significantly different from the cubic and higher wind speed dependences proposed by Callaghan et al. (2008, hereafter CAL08):

$$W = 3.18\times10^{-3}(U_{10}-3.70)^3; \qquad 3.70 < U_{10} \le 11.25 \text{ m s}^{-1}$$
$$W = 4.82\times10^{-4}(U_{10}+1.98)^3; \qquad 9.25 < U_{10} \le 23.09 \text{ m s}^{-1} \tag{2}$$

and Monahan and O'Muircheartaigh (1980, hereafter MOM80):

$$W(U_{10}) = 3.84\times10^{-4}U_{10}^{3.41} \tag{3}.$$

The MOM80 parameterization was derived on the basis of the data sets of Monahan (1971) and Toba and Chaen (1973). Most of the wind speed values from these two data sets are up to 12 m s^{-1} with only 10% of the data points for winds up to 19 m s^{-1}. The range of SST is from 17 to 31 °C. Monahan and O'Muircheartaigh (1986) emphasized that this is a regionally specific function, but its widespread adoption in global models led to its application at wind speeds and SSTs well beyond its range of validity.

In this study we explore the utility of the satellite-based W data from a standpoint of predicting SSA production rate. Whitecaps are used as a proxy for the amount of bubbles at the ocean surface. When these bubbles burst, they generate sea spray droplets which in turn transform to SSA when they equilibrate with the surroundings (Blanchard, 1983). Bursting bubbles produce film and jet droplets, whereas at high wind speeds, exceeding about 9 m s^{-1}, additional sea spray is directly produced as droplets which are blown off the wave crests (Monahan et al., 1983). These spume droplets are larger than the bubble-mediated SSA droplets (Andreas, 1992). In this study we will focus on bubble-mediated production of sea spray.

Sea spray aerosols are important for the climate system because, due to the vast extent of the ocean, SSA particles are amongst the largest aerosol sources globally (de Leeuw et al., 2011). SSA particles contribute to the scattering of short-wave electromagnetic radiation and

Deleted: and the subscripts denote the T_B frequencies used to obtain W

Deleted: above

thus to their direct radiative effect on climate. Also, having high hygroscopicity, SSA particles are a source for the formation of cloud condensation nuclei (Ghan et al., 1998; O'Dowd et al., 1999) and as such influence cloud microphysical properties and thus exert indirect radiative effects on the climate system. While residing in the atmosphere, SSA provide surface and volume for a range of multiphase and heterogeneous chemical processes (Andreae and Crutzen, 1997). Through such chemical processes, the SSA contribute to the production of inorganic reactive halogens (Cicerone, 1981; Graedel and Keene, 1996; Keene et al., 1999; Saiz-Lopez and von Glasow, 2012), participate in the production or destruction of surface ozone (Keene et al., 1990; Barrie et al., 1988; Koop et al., 2000), and provide a sink in the sulfur atmospheric cycle (Chameides and Stelson, 1992; Luria and Sievering, 1991; Sievering et al., 1992; 1995).

The modeling of all these processes in GCMs and CTMs starts with calculation of the production rate of SSA particles (termed also SSA production flux, SSA generation, or SSA emission). Sea spray source function (SSSF) is used to calculate SSA production flux—the number of SSA particles produced per unit of sea surface area per unit time. The most commonly used SSSF, proposed by Monahan et al. (1986, hereafter M86), estimates SSA emission by the indirect, bubble-mediated mechanism. Based on the discrete whitecap method, the SSSF of M86 is formulated in terms of $W(U_{10})$, as defined by MOM80 (Eq. (3)), whitecap decay timescale τ, and the aerosol productivity per unit whitecap dE/dr:

$$\frac{dF}{dr_{80}} = \frac{W(U_{10})}{\tau}\frac{dE}{dr_{80}} = 1.373 \cdot U_{10}^{3.41} \cdot r_{80}^{-3}(1 + 0.057 r_{80}^{1.05}) \times 10^{1.19e^{-B^2}}, \quad (4)$$

In Eq. (4), the timescale is a constant $\tau = 3.53$ s, r_{80} is the droplet radius at a relative humidity of 80%, and the exponent B is defined as $B = (0.38 - \lg r_{80})/0.65$. The term dE/dr, associated with the sea spray size distribution, determines the shape of the SSSF (i.e., shape factor); the term W/τ is a scaling (or magnitude) factor as it links predetermined SSA production per unit whitecap area with the amount of whitecapping in different regions at different seasons. Refer to Lewis and Schwartz (2004), de Leeuw et al. (2011), and Callaghan (2013) for clear distinction of the discrete whitecap method from the continuous whitecap method.

Estimates of SSA production fluxes using the discrete whitecap method still vary widely (Lewis and Schwartz, 2004; de Leeuw et al., 2011) precluding reliable estimates of the direct and indirect effects by SSA in GCMs, as well as the outcome of heterogeneous

chemical reactions taking place in and on SSA particles in CTMs. The wide spread of predicted SSA emissions is caused by a combination of uncertainties coming from both the magnitude and the shape factors of the used SSSFs. The uncertainties associated with the magnitude factor include difficulties of measuring W and τ and their natural variability, which affects the $W(U_{10})$ parameterizations. The assumptions of the discrete whitecap method (detailed in Sect. 2.4) also contribute to the uncertainty. Added to these are the uncertainties associated with the shape factor, such as its natural variability and the model chosen to parameterize the SSA size distribution. A source of uncertainty is the difficulty of directly measuring SSA fluxes which are used to develop and/or constrain SSSFs. When measurements of SSA concentrations are used to develop an SSSF, uncertainty comes from the deposition velocity model used to convert the concentrations to fluxes (e.g., Smith et al., 1993; Savelyev et al., 2014).

Aside from addressing uncertainties due to measuring techniques, there are two possible ways to improve the performance of a whitecap-based SSSF as regards the physical processes involved. One way is to address variations and uncertainties in the size-resolved productivity dE/dr_{80} (i.e., the shape factor in the SSSF), for instance by including the organic matter contribution to SSA at sub-micron sizes (O'Dowd et al., 2004; Albert et al., 2012) and/or by accounting for its variations with environmental factors instead of keeping it constant for all conditions (de Leeuw et al., 2011, Norris et al., 2013a; Savelyev et al., 2014). Another way is to address the variations and uncertainties in the whitecap fraction W (i.e., the magnitude factor in the SSSF) by steady improvements of the W measurements and by accounting for its natural variability. Both approaches are expected to reduce, or at least to better account for, the variations and uncertainties in parameterizing SSA flux.

Here we report on a study investigating the second of these two routes, namely—how using W data, which carry information for secondary factors, would influence the SSA production flux. The objective is to assess how much of the uncertainty in the SSA flux can be explained with the natural variability of W. Using the early version of the whitecap database (consisting of data for W_{10}, W_{37}, U_{10}, U_{dir} and T), we parameterize the W variability in terms of U_{10} and T. Our approach (Sect. 2) involves three steps. We first assess the satellite-based whitecap database to evaluate the wind speed dependence of W over as wide a range of U_{10} values as possible (sect. 3.1.1). In assessing the W database, we also evaluate the impact of an intrinsic correlation between W and U_{10}, which could have been introduced in

the process of estimating W from T_B (Sect. 3.1.2). The $W(U_{10})$ expression resulting from this analysis adjusts the trend of W with U_{10} to the concerted, globally-averaged influence of all secondary factors implicitly. We next apply the established $W(U_{10})$ expression to W data on regional scales in order to assess the variability caused by secondary factors in different locations during different seasons (Sect. 3.2). We analyze the regional fluctuations of W, remaining after the implicit adjustment with the $W(U_{10})$ expression, and parameterize them explicitly in terms of SST. The new $W(U_{10}, T)$ parameterization is compared to $W(U_{10})$ of MOM80 and SAL13 (Sect. 3.3) in order to assess to what extent SST can account for the W variability. Finally, the new $W(U_{10}, T)$ parameterization is used to estimate SSA emissions and compare results to previous predictions of SSA emissions (Sect. 3.4).

2 Methods

To achieve the study objective formulated above, the main task is to develop a parameterization of W that accounts for both the trend and the spread of the W data. Expressions $W(U_{10})$ model (predict) the trend of the whitecap fraction with wind speed. The inclusion of additional variables in $W(U_{10})$ relationships should be able to model (predict) the spread of the W data caused by natural variability. The approach described below aims at deriving an expression $W(U_{10}, T)$ that fulfils these two requirements.

2.1 Approach to derive whitecap fraction parameterization

Reasoning on a series of questions shaped our approach to parameterizing W and justified the choices we made for its implementation (Sect. 2.3). We first considered, Why do we need to parameterize W instead of using satellite-based W data directly? A major benefit of using satellite-based W data directly in an SSSF is that these data reflect the amount and persistence of whitecaps as they are formed by both primary and secondary forcing factors acting at a given location. This approach limits the uncertainty to that of estimating W from satellite measurements and does not add uncertainty from deriving an expression for $W(U_{10})$ or $W(U_{10}, T$, etc.). However, such an approach would limit global predictions of SSA emissions to monthly values because a satellite-based W data set does not provide daily global coverage; i.e., one would need data like those in Fig. 1a for at least two weeks (and more for good estimates of the uncertainties) in order to have full coverage of the globe.

Alternatively, a parameterization of whitecap fraction derived from satellite-based W data can provide daily estimates of SSA emissions using readily available daily data of wind

Deleted: wind speed dependence

Deleted: gain insights into the influence of

Deleted: In this second step, w

Deleted: use

Deleted: results of our

Deleted: . analysis to derive a new W parameterization that incorporates the effect of sea surface temperature (SST) T on W

Deleted: those

Deleted: , CAL08,

Deleted: shows

Deleted: The utility of

Deleted: evaluated by

Deleted: ing it

Deleted: ing

Deleted: What sets the new parameterization apart from previous parameterizations (e.g., MOM80 and SAL13) is its ability to model both the trend and the spread of the whitecap fraction with U_{10} and T. The implication is more realistic modeling and mapping of regional and seasonal variations of whitecap fraction. Salisbury et al. (2013) demonstrated the utility of the satellite-based whitecap database to Our study is a step further in using the for quantifying the influences of secondary factors ¶

Deleted: at

speed and other variables. Importantly, such a parameterization will be globally applicable because the whitecap fraction data cover the full range of meteorological conditions encountered over most of the world oceans. Because the availability of a large number of W data would ensure low error in the derivations of the $W(U_{10})$ or $W(U_{10}, T,$ etc.) expressions, we proceed with deriving a parameterization for W using the data in the whitecap database (Sect. 2.2.1).

The next question to consider was, How to account for the influence of secondary factors? Generally, to fully account for the variability of whitecap fraction, a parameterization of W would involve wind speed and many additional forcings explicitly to derive an expression $W(U_{10}, T,$ etc.) (MOM80; Monahan and Ó'Muircheartaigh, 1986; Anguelova and Webster, 2006). Using the early version of the whitecap database in this study, we start with parameterization $W(U_{10}, T)$.

Deleted: The SAL13 analysis showed substantial variations of W as a function of different variables, including SST. Because SST and wind speed are readily available variables, it would be useful to

The question that arises next is, How to combine the different dependences of W? One possibility is to use a single-variable regression to extract the W dependence on each variable separately, e.g., $W(U_{10})$ and $W(T)$. Then, these can be combined to derive an expression for their effects in concert, e.g., $W(U_{10}, T) = W(U_{10})W(T)$. While variables like T, atmospheric stability, surfactants, etc. influence W, they do not cause whitecapping. So a parameterization formulated with dedicated $W(T)$ and other expressions may put undue weight on such influences. This approach can be pursued when we have enough information to judge the relative importance of each influence (e.g., Anguelova et al., 2010, their Fig. 6) and include it in a combined expression with a respective weighting factor.

Previous experience points to another possibility to combine causal variables like U_{10} and influential variables like T and the likes. The Monahan and O'Muircheartaigh (1986) analysis of five data sets showed that the variability of W caused by SST (and the atmospheric stability) affect significantly the coefficients in the wind speed dependence $W(U_{10})$, especially the wind speed exponent. The survey of $W(U_{10})$ parameterizations by Anguelova and Webster (2006, their Tables 1 and 2) also clearly shows that each campaign conducted in different regions and conditions comes up with a specific wind speed exponent. This strongly suggests that the influence of secondary factors is implicitly expressed as a change of the wind speed

exponent. On the basis of their principal component analysis, SAL13 also suggested that in describing the W variability, it is more effective to combine individual variables with wind speed. On this ground, we proceed to obtain $W(U_{10}, T)$ as a wind speed dependence $W(U_{10})$ whose regression (or parametric) coefficients vary with SST.

How to realize this goal knowing that the satellite-based W data carry information for the effect of U_{10} and all other factors? One possible way to proceed is to: (i) express the mean trend in the W data associated with the globally-averaged conditions of U_{10} and all other factors; then (ii) quantify the fluctuations of regional W data around this mean trend as a function of a specific secondary factor. Here step (i) implicitly accounts for the effects of all secondary factors on W, while step (ii) quantifies explicitly the effect of a given factor on W. That is, the explicit formulation of the parametric coefficients accounts only partially for the full effect of a given secondary factor; it adds to the implicit account via the mean trend of W with U_{10}. To realize this concept, we first analyze the global W data set to identify a general wind speed dependence $W(U_{10})$ for the mean trend. Then, our analysis of regional W data helps to asses to what extent can SST account for the variations of the regression coefficients in a $W(U_{10})$ dependence.

The important question now is, What functional form should we use for the general (mean) $W(U_{10})$ dependence? Equations (1)-(3) exemplify the functional forms usually employed to express $W(U_{10})$:

$$W = aU_{10}^{n} \quad (5a)$$

$$W = a(U_{10} + b)^{3} \quad (5b).$$

A general $W(U_{10})$ dependence derived using Eq. (5a) would provide an empirical wind speed exponent n determined from available data sets, as MOM80 did using the available data sets at the time (Sect. 1). The wider the range of conditions represented by the data sets is, the closer the resulting $W(U_{10})$ dependence would be to average conditions globally and seasonally.

A general $W(U_{10})$ dependence derived using Eq. (5b) would provide a physically-based wind speed exponent n = 3 consistent with dimensional (scaling) arguments. Namely, because W is related to the rate at which the wind supplies energy to the sea, W should be

Deleted: his goal can be

Deleted: d

Deleted: by

Deleted: ing

Deleted: to use as a reference, then quantifying the variations of its regression coefficients in different regions and seasons

Deleted: reference

proportional to the cube of the friction velocity u_* (Monahan and O'Muircheartaigh, 1986; Wu, 1988). On this basis, Monahan and Lu (1990) related $W^{1/3}$ to U_{10} and derived the cubic power law in Eq. (5b). Subsequently, this relationship was used successfully in whitecap data analyses (e.g., Asher and Wanninkhof, 1998; CAL08). Coefficient b in Eq. (5b) is included because it is preferable for a $W(U_{10})$ relationship to involve a finite y-intercept (Monahan and O'Muircheartaigh, 1986). A negative y-intercept determines b from the x-intercept and is usually interpreted as the threshold wind speed for whitecap inception.

A modified version of Eq. (5) combines the merits of both formulations into the form:

$$W = a(U_{10} + b)^n \quad (6)$$

where the wind speed exponent is adjustable (i.e., a free parameter) and a finite y-intercept is included. A general $W(U_{10})$ dependence derived using Eq. (6) would provide a wind speed exponent as dictated by the whitecap database. Any of the three formulations (Eqs. (5 and 6)) can produce a viable general $W(U_{10})$ dependence, the empirical ones representative of the average conditions of the world oceans and the physical one supported by sound reasoning.

Moved (insertion) [1]

Deleted: that is applicable to all satellite-based W data. Being representative of globally averaged conditions, this general $W(U_{10})$ dependence can be applied with the same n to different regional scales and seasonal timeframes affording quantification of its variations with SST via coefficients a and b.

Moved up [1]: Any of the three formulations (Eqs. (5 and 6)) can produce a viable general $W(U_{10})$ dependence, the empirical one representative of the average conditions of the world oceans and the physical one supported by sound reasoning.

2.2 Data sets

To implement the approach thus formulated, we use the whitecap database on a global scale for the general $W(U_{10})$ dependence, and regional W subsets extracted from the whitecap database for the SST analysis. In describing the data sets used, we start with the whitecap database (Sect. 2.2.1). The considerations given to extract regional data sets from it are described in Sect. 2.2.2. We also introduce the data from the European Centre for Medium range Weather Forecasting (ECMWF) used in this study as an independent source to investigate possible intrinsic correlation among the entries of the whitecap database (Sect. 2.2.3).

2.2.1 Whitecap database

Anguelova and Webster (2006) describe in detail the general concept of retrieving the whitecap fraction W from measurements of the brightness temperature T_B of the ocean surface with satellite-borne microwave radiometers. Salisbury et al. (2013) describe the basic points of the retrieval algorithm estimating W (hereafter referred to as the $W(T_B)$ algorithm). Briefly,

the algorithm obtains W by using measured T_B data for the composite emissivity of the ocean surface and modelled T_B data for the emissivity of the rough sea surface and areas that are covered with foam (Bettenhausen et al., 2006; Anguelova and Gaiser, 2013). Minimization of the differences between the measured and modelled T_B data in the $W(T_B)$ algorithm ensures minimal dependence of the W estimates on model assumptions and input parameters. An atmospheric model is necessary to evaluate the contribution from the atmosphere to T_B.

Wind speed U_{10} is one of the required inputs to the atmospheric, roughness and foam models (Anguelova and Webster, 2006; Salisbury et al., 2013). Wind speed data come from the SeaWinds scatterometer on the QuikSCAT platform or from the Global Data Assimilation System (GDAS), whichever matches up better with the WindSat data in time and space within 60 min and 25 km; hereafter we refer to both QuikSCAT or GDAS wind speed values as U_{10} from QuikSCAT or $U_{10QSCAT}$. The use of $U_{10QSCAT}$ in the estimates of satellite-based W is anticipated to lead to some intrinsic correlation when/if a relationship between W and $U_{10QSCAT}$ is sought.

Deleted: 25 km and

The W data used in this study are obtained from T_B at 10 and 37 GHz, W_{10} and W_{37}; data for 37 GHz are shown in Fig. 1a. The W_{10} and W_{37} data approximately represent different stages of the whitecaps because of different sensitivity of microwave frequencies to foam thickness (Anguelova and Gaiser, 2011). Data W_{10} are an upper limit for predominantly active wave breaking (stage A whitecaps (Monahan and Woolf, 1989)) partially mixed with decaying (stage B) whitecaps, while W_{37} data quantify both active and decaying whitecaps. Because decaying foam covers a much larger area of the ocean surface than active whitecaps (Monahan and Woolf, 1989), W_{37} data are usually larger than W_{10} data. Comparisons to historic and contemporary in situ W data in Fig. 1b confirm the approximate representations of stage A whitecaps (cyan squares) and A + B whitecaps (blue diamonds) by W_{10} (green) and W_{37} (magenta), respectively. Anguelova et al. (2009) have quantified the differences between satellite-based and in situ W data using both previously published measurements and time-space match-ups of W and discussed possible reasons for the discrepancies.

The satellite-based W data are gridded into a 0.5°×0.5° grid cell together with the variables accompanying each W data point, namely $U_{10QSCAT}$, T from GDAS, time (average of the times of all samples falling in each grid cell), and statistical data generated during the gridding including the root-mean-square (rms) error, standard deviation (SD), and count (the number of individual samples in a satellite footprint averaged to obtain the daily mean W for a

grid cell). In this study, we used daily match-ups of W, U_{10}, and T data for each grid cell for the year 2006. To reiterate, this data set—consisting of W_{10} and W_{37} accompanied with three environmental variables (U_{10}, U_{dir} and T)—is an early version of the whitecap database; the extended W database used by SAL13 (Sect. 1) contains three additional variables suitable to quantify explicitly the effects of wave field and atmospheric stability on W. Due to large data gaps in both space and time, the daily W data cannot be interpolated to provide better coverage (Fig. 1a). Therefore, only the available data are used without filling the gaps for areas where data are lacking. This global data set was used to assess the globally averaged wind speed dependence of W.

2.2.2 Regional data sets

The annual global W distributions show regions with valid data points ranging from 100 to 300 samples per grid cell per year when both ascending and descending satellite passes are considered. Thus, different regions were selected using two criteria, namely (i) consider regions with a high number of valid data points, and (ii) obtain a selection representative of different conditions in the northern and southern hemispheres (NH and SH).

Deleted: There are fewer samples for latitudes beyond 60°S or N (see Fig. 1a) because WindSat and QuikSCAT have fewer matching points there (Sect. 2.2.1).

With these criteria, 12 regions of interest were selected (Fig. 2) and W, U_{10}, and T data for each region were extracted from the whitecap database. The coordinates of the selected regions are listed in Table 1, together with the corresponding number of samples and minimum, maximum, mean, and median values for wind speed and SST for January and July. For 90% of the regional and monthly data used in the study, the percent difference (PD, defined as the difference between two values divided by the average of the two values) between mean and median values of U_{10} and T is less than 4% and 9.5%, respectively. With medians and means approximately the same, the U_{10} and T data have normal distributions; i.e., outliers, though existing, do not affect the mean values significantly. All analyses presented here use the mean U_{10} and T values. Figure 3 shows the seasonal cycles of the mean U_{10} and T values for four of the selected 12 regions visualizing the full range of U_{10} and T data (Table 1).

Regions 2-11 are all in the open ocean; region 1 was selected for its landlocked position. Region 6 in the Pacific Doldrums is used as a reference for the lower limit of U_{10} (Fig. 3a), while region 12 is included to represent the lowest T values (Fig. 3b). Four regions (2, 3, 7, and 8) are at latitudes between 0 and 30°S and N (Tropics and Subtropics)

Deleted: ,

representing the Trade winds zone. These are regions with persistent (Easterly) winds blowing over approximately the same fetches (except region 8) in oceans with different salinity (Tang et al., 2014) and primary production (Falkowski et al., 1998) (a proxy for surfactant concentrations). Region 4 is in the NH temperate zone representing long-fetched Westerly winds. Region 5 covers the latitudes between 40°S and 50°S known as "The Roaring Forties" for the strong Westerly winds there, but is characterized with shorter fetch. Differences in the seasonal cycles of U_{10} and T in regions 4 and 5 (Fig. 3) suggest more uniform conditions and longer fetches in the SH temperate zone. We have chosen regions 8 and 9 to represent different zonal conditions and to gauge the effect of narrower range of SST variations (as compared to the SST range in region 5). Chosen at the same latitude, regions 9-11 have approximately the same SST, salinity, and surfactants but represent different wind fetches, shortest for region 9 and longest for region 11. Overall, the chosen regions cover the full range of global oceanic conditions and, while representative of diverse regional conditions, each one has distinct regional characteristics.

Deleted: are

2.2.3 Independent data source

Ideally, when deriving a $W(U_{10})$ parameterization, the data for W and U_{10} should come from independent sources. The intrinsic correlation between W and U_{10} that might have arisen from the use of U_{10} from QuikSCAT in the estimates of W from T_B (Sect. 2.2.1), might affect the relationship between W and U_{10} developed here. To evaluate the magnitude of such intrinsic correlation, we used U_{10} from the ECMWF ($U_{10\mathrm{ECMWF}}$), which is considered to be a more independent source. Note though that even the ECMWF data are generated by assimilating observational data sets (e.g., from buoys) in a coupled atmosphere-wave model (Goddijn-Murphy et al., 2011).

To compile this "independent" data set, we made time-space matchups between the W_{10} and W_{37} data and $U_{10\mathrm{ECMWF}}$ from the 3-hourly ECMWF data for 2006. For each W–$U_{10\mathrm{QSCAT}}$ pair at a time t from the original W database, there is a corresponding W–$U_{10\mathrm{ECMWF}}$ pair of data within an interval $t \pm 1.5$ h. This matching procedure differs from the W–$U_{10\mathrm{QSCAT}}$ matching which was done at the WindSat swath resolution, before gridding the variables for the whitecap database. To speed up calculations, and because this already provides a statistically significant amount of data, we used only ascending satellite overpasses. Wind

Deleted: In this way, f

speeds above 35 m s^{-1} were discarded. Besides ECMWF wind data, for consistency we also extracted ECMWF SST values.

Figure 4a shows all ECMWF wind speed data that have been matched in time and space with the available $U_{10QSCAT}$ data for March 2006. The majority of the data is clustered in the range of 5-10 m s^{-1} (dark red). To characterize the difference between the two wind speed sources, the correlation between U_{10} from ECMWF and U_{10} from QuikSCAT was determined as the best linear fit forced through zero:

$$U_{10_{ECMWF}} = 0.952 U_{10_{QSCAT}} \quad (7)$$

with a coefficient of determination $R^2 = 0.844$. For comparison, the unconstrained fit between $U_{10QSCAT}$ and $U_{10ECMWF}$ is also shown in Fig. 4a (dashed line); both fits are very close (they almost overlap) with almost identical correlation coefficients (R^2 = 0.845 for the unconstrained fit). Similarly, Fig. 4b compares T from ECMWF and GDAS showing almost 1:1 correlation. That is, the two data sources provide almost the same values for T.

On average, U_{10} from ECMWF is about 5% lower than U_{10} from QuikSCAT. This U_{10} difference can be explained to some extent with the effect of atmospheric stability because QuikSCAT provides equivalent neutral wind which accounts for the stability effects on the wind profile (Kara et al., 2008; Paget et al., 2015), while the ECMWF model gives stability dependent wind speeds (Chelton and Freilich, 2005).

Having the correlation between U_{10} from the whitecap database and U_{10} from the ECMWF quantified (as well as for T), one can evaluate differences caused by the use of different data sources. Equation (7) could also be useful when one decides to use ECMWF data because of their availability at 6 or 3 h intervals as compared to the availability of W, U_{10}, and T match-ups twice a day (Sect. 2.2.1).

Deleted: s

Deleted: and T

2.3 Implementation

We aim to develop an expression capable of modeling both the trend of the satellite-based W data with U_{10} and their spread (see green and magenta symbols in Fig. 1b). We first analyze the satellite-based W data to derive a general $W(U_{10})$ expression (i.e., the trend of W with U_{10}). We apply Eq. (6) with coefficients (n, a, b) left as free parameters to global data sets of W_{10}, W_{37}, and both together (W_{10} & W_{37}). Table 2 shows the results for the regression coefficients with their SDs from the fitting procedure. Each set of coefficients accounts implicitly for U_{10}

Deleted: of the satellite-based W data

Deleted: global data sets of

Deleted: W_{10} and W_{37} data and

Deleted: that represents average wind conditions in different geographical environments

and all secondary factors to a deferent degree for different data sets. However, to consistently interpret and explicitly quantify regional and seasonal variations of W data, it is necessary to analyze all W data—global, regional and at different frequencies—with the same mean trend given by the $W(U_{10})$ expression. Significance t-tests shows that the wind speed exponents n determined as free parameters (Table 2) are not statistically different from $n = 2$ ($p > 0.05$). On this ground, we set $n = 2$ and for all subsequent analyses we use a functional form modified from Eq. (6):

$$W = a(U_{10} + b)^2 \quad (8a).$$

Following Monahan and Lu (1990), we derive an expression $W(U_{10})$ in the form of Eq. (8a) by plotting $W^{1/2}$ as a function of $U_{10QSCAT}$. Applying linear regression, we find an expression:

$$W^{1/2} = mU_{10} + c \quad (8b)$$

which is then rearranged and squared to provide coefficients $a = m^2$ and $b = c/m$ in Eq. (8a) (results in Sect. 3.1.1). All linear fits are done on the W data associated with U_{10} from 3 to 20 m s^{-1}. The lower limit of 3 m s^{-1} is chosen as a threshold for observing whitecaps. This restriction is reasonable in light of the SAL13 analysis in which W data with a relative standard deviation $(\sigma_W / W) > 2$ were removed: the discarded W data were about 10% of all W data, mostly in regions with low wind speeds of around 3 m s^{-1}. We exclude the high wind speed regime in order to avoid uncertainty due to (i) fewer data points in this regime; and (ii) anticipated larger uncertainty in the W data from the $W(T_B)$ algorithm.

For the intrinsic correlation analysis, the W–$U_{10ECMWF}$ data pairs are used in a similar fashion to make $W^{1/2}(U_{10ECMWF})$ linear fits and derive from them a relationship between the satellite-based W data and the ECMWF wind speeds. The two global $W(U_{10})$ parameterizations for the two wind speed sources are then compared to evaluate the magnitude of the intrinsic correlation (results in Sect. 3.1.2).

Because Eq. (7) gives the possibility to evaluate discrepancies due to the use of different sources for U_{10} and T, we use U_{10} and T from the whitecap database in all subsequent analyses and results. In this way, with the intrinsic correlation characterized, we restrict the uncertainty in our analyses by using the close matching-up of W, U_{10}, and T data in the whitecap database. This decision is reasonable considering that both data sets can be used

Field Code Changed

Deleted: 6

Deleted: raised to the power n

Deleted: ing

Deleted: m^n

Deleted: 6

Deleted: points

Deleted: . T

Deleted: With the wind speed threshold imposed in this way, we propose a broader interpretation of regression coefficient b (sect. 3.1.1).

Deleted: n

in practice for different applications. The collocated data in the whitecap database (involving QuikSCAT) are most handy for analysis (as done in this study). Meanwhile, W data from the whitecap database combined with forcing data from a global model (such as ECMWF or other) are useful for forecasts and climate simulations.

With $n = 2$ for the general wind speed dependence determined, we then apply Eq. (8b) to the regional monthly sub-sets of W_{10} and W_{37} data. All available data per month were used, ranging from 22 to 31 days of data. Once again, scatter plots of $W^{1/2}(U_{10})$ were generated and the best linear fits were determined providing coefficients m and c for each region for each month for W_{10} and W_{37}. The regional and seasonal variations of coefficients a and b are analyzed to inform us how to parameterize them in terms of SST, $a(T)$ and $b(T)$ (results in Sect. 3.2). To quantify how $a(T)$ and $b(T)$ are influenced by different wind speed dependences—our empirically determined wind speed exponent $n = 2$ (Eq. (8a)) or the physically reasoned cubic wind speed dependence (Eq. (5b))—we also analyzed scatter plots of $W^{1/3}(U_{10})$ and derived a respective set of coefficients $a(T)$ and $b(T)$. We quantify differences between new and previously published parameterizations with two metrics (results in Sect. 3.3): (i) the PD between W values obtained with different parameterizations; and (ii) significance tests (Student t-test and ANOVA) of the differences between W values obtained with new and previous W parameterizations.

Efforts to include wave parameters in W parameterizations are well justified because, after wind speed, the most important secondary factor that accounts for variability in W is the wave field (SAL13). Lacking wave characteristics, the early version of the whitecap database is not suitable for deriving an explicit expression for the wave field influence on W. However, we have investigated the effect of rising and waning winds on the $W(U_{10})$ relationship; increasing-decreasing winds are considered a proxy for undeveloped-developed seas (Stramska and Petelski, 2003; CAL08). It is not feasible to determine whether winds are rising or waning from satellite-based wind speed data because of their low temporal resolution: twice a day at a given location. As wind speed provided by ECMWF is available every three hours, $U_{10ECMWF}$ values were used to examine the wind conditions at the satellite overpass time associated with a W data point. Wind speed difference between two three-hours intervals ΔU_{10} has been used to detect changing winds. Wind speed differences ΔU_{10} from of 1 to 5 m s^{-1} in steps of 1 m s^{-1} were used to examine the sensitivity of the analysis to the choice of ΔU_{10} in identifying rising or waning winds. Higher ΔU_{10} values are associated with

Deleted: 6

Deleted: with the same *n*

Deleted: n

Deleted: *m* and *c*, as well as

Deleted: ,

Deleted: judge to what extent these variations warrant

Deleted: ation

Deleted: ¶

Deleted: the functional form of the general

Deleted: 6

Deleted: and

Deleted: We analyzed the variations of coefficients *m* and *c* with the Student's T-statistics and Analysis of variance (ANOVA) tests. The Student test verifies whether two data sets (or sample populations) have significantly different means by confirming or rejecting the null hypothesis (the default statement that there is no difference among data sets). A small significance value (e. g., $p < 0.05$) for any pair of regional *m* and *c* data sets would indicate that the regional means of coefficients *m* and *c* are significantly different. The ANOVA test essentially does the same but for a group of three or more data sets simultaneously. ANOVA rejects the null hypothesis if two or more populations differ with statistical significance. In this sense, an ANOVA test is less specific than a Student test. Because the ANOVA assumptions (that the data sets are normally distributed and they have approximately equal variances) may not always be true for our data, the ANOVA results were verified with the more general Kruskal-Wallis H test (referred to as H test) which does not have any of these assumptions. ¶

Deleted: ,

Deleted: , and H

Moved (insertion) [2]

Deleted: B

Deleted: , efforts to include wave parameters in *W* parameterizations are well justified

Moved (insertion) [3]

Deleted: For completeness

Deleted: also

Deleted: either

Deleted: or

Deleted: as

the passage of stronger atmospheric low-pressure systems, which come with higher wind speeds and thus stronger wind forcing of waves. The $U_{10QSCAT}$ values were correlated with W using Eq. (8). Only data for 37 GHz from the ascending satellite overpass were used.

2.4 Estimation of sea spray aerosol emissions

The newly formulated $W(U_{10}, T)$ parameterization is applied to estimate the global annual SSA emission using SSSF of M86 (Eq. (4)). Dividing Eq. (4) by Eq. (3), we modify the M86 SSSF to clearly separate the magnitude and shape factors (re-written here as Eq. (4′)):

$$\frac{dF}{dr_{80}} = W(U_{10},T)\cdot\left[3.5755\times10^{5}\cdot r_{80}^{-3}(1+0.057r_{80}^{1.05})\times10^{1.19e^{-B^2}}\right] \qquad (4')$$

with B as defined in Sect. 1; with this re-arrangement, the timescale τ is absorbed in the shape factor (the expression in the brackets). The size range for M86 validity is r_{80} = 0.8–8 μm. We calculate the SSA flux for radii r_{80} ranging from 1 to 10 μm. Refer to Anguelova (2016) for using the $W(U_{10})$ parameterization of SAL13 to estimate CO_2 transfer velocity and SSA flux for r_{80} ranging from 0.4 to 250 μm.

2.4.1 Use of discrete whitecap method

The main assumptions of M86 for the SSSF based on the discrete whitecap method—constant values for τ and dE/dr (Sect. 1)—are usually questioned (Lewis and Schwartz, 2004; de Leeuw et al., 2011; Savelyev et al., 2014). It is not expected for both of these assumptions to hold for wave breaking at various scales and under different conditions in different locations. The SSSF proposed by Smith et al. (1993) on the basis of measured size-dependent aerosol concentrations is one of the first formulations to demonstrate that the shape factor cannot be constant. Norris et al. (2013a) also demonstrated that the aerosol flux per unit area whitecap varies with the wind and wave conditions.

Recently, Callaghan (2013) showed that the whitecap timescale is another source of often overlooked variability in SSSF parameterizations based on M86. Because W typically includes foam from all stages of whitecap evolution, Callaghan (2013) suggested that the adequate timescale for the aerosol productivity from a discrete whitecap is not just its decay time (as in Eqs. (4) and (4′)), but the sum of the whitecap formation and decay timescales τ'. The value of τ' varies from breaking wave to breaking wave, but an area-weighted mean

Deleted: and

Deleted: basic

whitecap lifetime can be calculated for any given observational period to account for this natural variability. Analyzing the lifetimes of 552 oceanic whitecaps from a field experiment, Callaghan (2013) found that the area-weighted mean τ' varies by a factor of 2.7 (from 2.2 to 5.9 s). We refer the reader to Callaghan (2013) for an SSSF that accounts for SSA flux variability by explicitly incorporating whitecap timescale τ'.

Despite these questionable assumptions, the SSSF based on the discrete whitecap method in the form of M86 has been widely used in many models (Textor et al., 2006). Therefore, to those who have worked with M86 until now, a meaningful way to demonstrate how the new satellite-based *W* data, and *W* parameterizations based on them, would affect estimates of SSA flux is to hold everything else constant (e.g., the whitecap timescale and productivity in the shape factor) and clearly show differences caused solely by the use of new *W* expression(s) as a magnitude factor. On these grounds, the choice of the SSSF based on the M86 whitecap method is a suitable baseline for comparisons.

2.4.2 Choice of size distribution

Though the chosen size range of 1–10 μm for SSA particles is limited, it is well justified for the purposes of this study with the following arguments.

Generally, the division of the SSA particles into sizes of small, medium, and large modes (de Leeuw et al., 2011, their §8) is well warranted when one considers the climatic effect to be studied (Sect. 1). For example, sub-micron particles are important for scattering by SSA (direct effect) and the formation of cloud condensation nuclei (indirect effect), while super-micron particles are important for heat exchange (via sensible and latent heat fluxes) and heterogeneous chemical reactions (which need surface and volume to proceed effectively). However, in this study we do not focus on how the choice of the size distribution will affect the SSA estimates. Nor do we aim to present estimates of specific effect on the climate system. Rather, with a fixed size distribution, we explore how parameterizing *W* data, which carry information for the influences of many factors, would affect estimates of SSA emission (Sect. 1). In this sense, we can choose to use any published size distribution as a shape factor.

The chosen size range is the range of medium (super-micron) mode of SSA particles. This is the range for which the size distribution of M86 is valid (Sect. 2.4). The M86 size distribution, in its original or modified form, is widely used in GCMs and CTMs (Textor et

al., 2006, their Table 3). The size range of 1–10 μm is a recurrent part of the various size ranges used in all (or at least most) SSSFs (see Table 2 in Grythe et al. (2014, hereafter G14)).

The chemical composition of the SSA particles is another argument favoring the chosen size range. The super-micron particles consist, to a good approximation, solely of sea salt, whereas, in biologically active regions, the sub-micron size range additionally includes organic material, with an increasing contribution as particle size decreases (O'Dowd et al., 2004, Facchini et al., 2008; Partanen et al., 2014). Since the organic mass fraction in sub-micron SSA particles is still highly uncertain (Albert et al., 2012), we focus on the medium mode SSA emissions.

We evaluate the discrepancy expected due to neglecting particles below 1 μm using the G14 report of SSA production rate for dry particle diameters $D_p = r_{80}$ obtained with M86 over two different size ranges: 4.51×10^{12} kg yr^{-1} for the size range of 0.8 μm < r_{80} < 8 μm and 5.20×10^{12} kg yr^{-1} for size range of 0.1 μm < r_{80} < 10 μm. The different size ranges bring a difference between the two G14 estimates of about 14%. Neglecting particles with r_{80} < 0.1 μm would not change significantly the results presented here because they contribute on the order of 1% to the overall mass (Facchini et al., 2008).

Because total whitecap fraction, rather than only the active breaking crests, provides bubble-mediated production of SSA, we use W_{37} data to estimate the emission of medium mode SSA. The calculations use a modeling tool (Albert et al., 2010) in which the $W(U_{10})$ parameterization of MOM80, as integrated in Eq. (4), was replaced with the newly derived $W(U_{10}, T)$ parameterization (Eq. (4′)). The resulting size-segregated droplet number emission rate was converted to mass emission rate using the approximation $r_{80} = 2r_d \equiv D_p$, where r_d and D_p are the particle dry radius and diameter, respectively (e.g., Lewis and Schwartz, 2004; de Leeuw et al., 2011), and a density of dry sea salt of 2.165 kg m^{-3}.

3 Results and Discussion

The graphs visualizing our results use all W data available for wind speeds from 3 to 35 m s^{-1}. This range of U_{10} is beyond the range $3 \le U_{10} \le 20$ m s^{-1} used for all fits (Sect. 2.3). In addition, the QuikSCAT instrument, which provided the U_{10} satellite data used in this study, has a decreased sensitivity for wind speeds over 20 m s^{-1} (Quilfen et al., 2007). All results regarding higher wind speeds should, therefore, be handled with caution.

Deleted: is

Deleted: showing

Deleted: visualize the

Deleted: points

Deleted: 0

Deleted: , but

Deleted: are valid for $3 \le U_{10} \le 20$ m s^{-1}

Moved (insertion) [4]

Deleted: At the same time

3.1 Global data analysis

Figure 5 shows global W data estimated from WindSat measurements for March 2006 as function of $U_{10QSCAT}$ with linear and logarithmic y-axes at 10 GHz (Fig. 5a and c) and 37 GHz (Fig. 5b and d). For comparison, the MOM80 relationship (Eq. (3)) is also plotted in each panel. There are three noteworthy observations in Fig. 5. First, we note the different variability of W_{10} and W_{37} data. The 10 GHz data show far less variability than those at 37 GHz. The W_{37} data at a certain wind speed vary over a much wider range, with the strongest variability for wind speeds of 10-20 m s^{-1}. This supports the suggestion that other variables, in addition to U_{10}, influence the whitecap fraction, such as SST or wave field; SAL13 analyzed this variability.

Another observation in Fig. 5 is noted at low wind speeds. The 10 GHz scatter plots do not show W data for wind speeds lower than about 2 m s^{-1} because at these low wind speeds no active breaking occurs (Sect. 1). In contrast, non-zero W_{37} data are retrieved at wind speeds $U_{10} < 2$ m s^{-1}. Salisbury et al. (2013) suggested that the presence of foam on the ocean surface at these low wind speeds could be due to residual long-lived foam. This residual foam might be stabilized by surfactants, which increases its lifetime (Garrett, 1967; Callaghan et al., 2013). Another explanation could be production of bubbles and foam from biological activity (Medwin, 1977). However, there is not enough information currently to prove any of these conjectures.

The comparison of the MOM80 relationship (Eq. (3)) to W_{10} and W_{37} data clearly reveals the most important feature in Fig. 5 (red curves)—the wind speed dependence of satellite-based W data deviates from cubic and cubic-like relationship.

3.1.1 Wind speed dependence

Following the arguments of our approach (Sect. 2.1) and evaluating the wind speed exponents determined as free parameters (Table 2), we found that a quadratic wind speed exponent (n = 2) fits reasonably well both W_{10} and W_{37} data sets. For the same data shown in Fig. 5, Fig.6 shows the linear regression of the square root of W versus U_{10}:

$$W^{1/2} = 0.01U_{10} - 0.011 \qquad 10\ \text{GHz} \qquad (9a)$$

$$W^{1/2} = 0.01U_{10} + 0.019 \qquad 37\ \text{GHz} \qquad (9b)$$

Deleted: Parameterization from g

Deleted: set

Deleted: ,

Deleted: quantify

Deleted: es

Deleted: trying different expressions

Deleted: best

with coefficients of determination R^2 of 0.996 and 0.951, respectively. From Eq. (9), we obtain the following global average wind speed dependence of W using U_{10} from QuikSCAT:

$$W_{10} = 1\times10^{-4}\left(U_{10} - 1.1\right)^2 \quad (10)$$

$$W_{37} = 1\times10^{-4}\left(U_{10} + 1.9\right)^2 \quad (11)$$

where W is a fraction (not %).

The finding of weaker (quadratic) wind speed dependence here is not unprecedented. The first reported $W(U_{10})$ relationship of Blanchard (1963) was quadratic. With careful statistical considerations, Bondur and Sharkov (1982) derived a quadratic $W(U_{10})$ relationship for residual W (strip-like structures, in their terminology). Parameterizations of W in waters with different SST have also resulted in wind speed exponents around 2 (see Table 1 in Anguelova and Webster, 2006).

Quadratic wind speed dependence is also consistent with the wind speed exponents of SAL13 in Eq. (1). The PD between our quadratic $W(U_{10})$ and SAL13 $W(U_{10})$ at 37 GHz ranges from 0.5% to 10% over the wind speed range of 3–20 m s^{-1}. ANOVA and Student tests show that these differences are not statistically significant. That is, the global quadratic $W(U_{10})$ parameterization approaches the predictions of the SAL13 parameterization, which has a more specific wind speed exponent (n = 1.59). Note that we do not expect our $W(U_{10})$ parameterization to be distinctly different from that of SAL13 because both studies use the same data for W and U_{10} (though from different versions of the whitecap database). Rather, we aim to identify general $W(U_{10})$ trend in order to perform consistent regional analysis.

The y-intercept for W_{10} (Eq. (10)) is negative and, following the usual interpretation, yields a threshold wind speed of 1.1 m s^{-1} for whitecap inception. This is in the range of previously published values from 0.6 (Reising et al., 2002) to 6.33 (Stramska and Petelski, 2003). Meanwhile, the positive y-intercept b for W_{37} (Eq. (11)) is meaningless at first glance and intriguing upon some pondering. While stabilized residual foam and/or foam from biological sources are possible (Sect. 3.1), it is not known whether such mechanisms are capable of providing a measurable amount of foam patches which produce bubble-mediate sea spray efficiently.

We propose broader interpretation of b in Eqs. (10-11), be it negative or positive. Generally, it is expected that the atmospheric stability (Kara et al., 2008) and fetch (through

Deleted: correl

Deleted: a

Moved (insertion) [5]

Deleted: the global

Deleted: such

Deleted: replicates

Deleted: trend

Deleted: the satellite-based W data as well as

Deleted: database

Deleted: is

Deleted: is

the wave growth and development) cause inception of the whitecaps at lower or higher wind speed. One can consider the range of values for b mentioned above (0.6 to 6.33) as an expression of such influences. We suppose that b can also incorporate the effect of the seawater properties on the extent of W. The net result of all secondary factors may be either negative or positive b.

Specifically, we promote the hypothesis that a positive y-intercept b can be interpreted as a measure of the capacity of seawater with specific characteristics, such as viscosity and surface tension—which are governed by SST, salinity, and surfactant concentration—to affect W. Undoubtedly, none of these secondary factors creates whitecaps per se. Rather, they prolong or shorten the lifetime of the whitecaps via processes governed by the seawater properties. For instance, surfactants and salinity influence the persistence of submerged and surface bubbles. This yields variations of bubble rise velocity that replenish the foam on the surface at different rates. Long-lived decaying foam added to foamy areas created by subsequent breaking events would augment W; conversely, conditions that shorten bubble lifetimes would reduce W (or at least not add to W).

A positive y-intercept can be thought of as a mathematical expression of this static forcing (as opposed to dynamic forcing from the wind) that given seawater properties can sustain. That is, at any given location, this static forcing acts as though higher wind speed of magnitude (U_{10} + b) is producing more whitecaps than U_{10} alone. By parameterizing coefficients a and b in terms of different variables, one can evaluate how much the static forcing affects W in different geographic regions. By developing parameterizations $a(T)$ and $b(T)$ (Sect. 2.1), here we quantify only one static influence.

The rise-wane wind effect, as detected in this study (Sect. 2.3), is not pronounced compared to findings in previous studies that use in situ wind speed data. Goddijn-Murphy et al. (2011) studied wind history and wave development dependencies on in situ W data using wave model (ECMWF), satellite (QuikSCAT), and in situ data for U_{10}. These authors detected significant effects only with in situ U_{10}. The limited wave field effect in our study might be traced back to the method through which U_{10} was determined: wind speeds from satellites are spatial averages of scatterometric or radiometric observations that take a snapshot of the surface as it is affected by both history and local conditions, whereas in situ data for wind speed are single point values averaged over a short time and hence representative for a relatively small area. The effect of the spatial averaging of the satellite

Deleted: ggest

Deleted: es

Moved up [3]: For completeness, we have also investigated the effect of either rising or waning winds on the $W(U_{10})$ relationship; increasing-decreasing winds are considered as a proxy for undeveloped-developed seas (Stramska and Petelski, 2003; CAL08).

Deleted: absence of a significant wind history

Deleted: therefore

data over a much larger area (i.e., the satellite footprint) might be that information on wind history is lost in the process. Limited results on the effect of the wave field obtained with a proxy analysis of the wind history do not justify further consideration in this study.

3.1.2 Intrinsic correlation

To quantify the possible intrinsic correlation in the derived $W(U_{10})$ parameterization (Eqs. (10-11)), we derived $W(U_{10})$ using ECMWF wind speeds instead of the QuikSCAT wind speeds (Sect. 2.3). Figure 7a shows a scatter plot of $W^{1/2}$ versus $U_{10\mathrm{ECMWF}}$ (only data for 37 GHz are shown); dashed and solid lines show unconstrained and zero-forced fits, respectively. The linear regression (given in the figure legend) is used to obtain the global average wind speed dependence using U_{10} from ECMWF as follows:

$$W_{37} = 8.1\times10^{-5}\left(U_{10}+3.33\right)^2 \qquad (12).$$

The positive intercept here is interpreted as in Sect. 3.1.1. Using Eq. (12), parameterized W values are plotted as a function of $U_{10\mathrm{ECMWF}}$ in Fig. 7b. Increased scatter of the W data is evident when comparing Figs. 7b and 5d. We use different metrics to detect and evaluate possible intrinsic correlation.

The change of the coefficient of determination R^2 of the $W(U_{10})$ relationship when QuikSCAT winds are substituted with the ECMWF winds is one sign for the presence of intrinsic correlation. Physically, we expect a strong correlation between W and U_{10}, and we see this clearly in Fig. 6b which shows R^2 = 0.951 for $W^{1/2}$ and $U_{10\mathrm{QSCAT}}$. However, the correlation coefficient might not be as high as in Fig. 6 if U_{10} were from a more independent source. We see this when comparing Figs. 6b and 7a. The $W^{1/2}$–U_{10} correlation is still strong in Fig. 7a, but the plot shows more scatter and slightly lower correlation with R^2 = 0.826.

Figure 8 visualizes the change in the spread of the W data with a plot of the residuals (biases) between the W data and the derived W parameterizations (Eqs. (11) and (12)) as a function of wind speed; Fig. 8a is for $U_{10\mathrm{QSCAT}}$ and Fig. 8b is for $U_{10\mathrm{ECMWF}}$. Larger biases are evident when $U_{10\mathrm{ECMWF}}$ is used. The root-mean-square deviation between W data and parameterized W values increases from ΔW = 0.214% for the data set using $U_{10\mathrm{QSCAT}}$ to ΔW = 0.367% for the data set using $U_{10\mathrm{ECMWF}}$.

The slopes in Figs. 6b and 7a differ by about 11%. We evaluate how this translates into differences in W_{37} values as predicted by Eqs. (11) and (12). We found the PD between $W_{37}(U_{10\mathrm{QSCAT}})$ and $W_{37}(U_{10\mathrm{ECMWF}})$ to be less than ± 9% for wind speeds of 7–23 m s^{-1}.

Deleted: T

Deleted: , therefore, is

Deleted: sought

Deleted: T

Deleted: the significance of the

Deleted: , we look at

Deleted: t

Deleted: correlation

Deleted: $W^{1/2}$

Deleted: a correlation coefficient

Deleted: This is a sign that probably some intrinsic correlation contributes to the $W(U_{10\mathrm{QSCAT}})$ relationship which, therefore, is stronger than $W(U_{10\mathrm{ECMWF}})$.

Deleted: using

Specifically, the W_{37} values obtained with $U_{10QSCAT}$ and $U_{10ECMWF}$ are equal for wind speed of 11 m s^{-1}. Below 11 m s^{-1}, $W_{37}(U_{10ECMWF})$ is higher than $W_{37}(U_{10QSCAT})$ by up to 8.8%. Above 11 m s^{-1}, $W_{37}(U_{10ECMWF})$ is smaller than $W_{37}(U_{10QSCAT})$ by up to 8.4%. The difference goes up to 30% for wind speeds of 3 m s^{-1}.

While different metrics suggest that the intrinsic correlation is present and may contribute to these differences, it is not the only reason for the discrepancies. Different matching procedures (Sect. 2.2.3) and the difference of about 5% between the U_{10} values from the two different sources (Fig. 4a) also contribute to the W discrepancies from Eqs. (11) and (12). We, therefore, conclude from the PD values that the effect of the intrinsic correlation alone on W is most likely less than about 4% for most wind speeds.

Deleted: R^2 values for the regressions in Figs. 6b and 7

Deleted: this

Deleted: possible

Deleted: T

Deleted: s

Deleted: Of course, we have to consider these differences in the light of other uncertainties in Eqs. (11) and (12) such as the uncertainties in determining $U_{10QSCAT}$ and $U_{10ECMWF}$ and the satellite-based W data itself.

3.2 Regional and seasonal data analyses

The wind speed exponent in the $W(U_{10})$ relationship derived from the global data set (Eqs. (10-11)) implicitly accounts for the globally-averaged effects of all secondary factors affecting the satellite-based W data. Now we apply Eq. (8) to regional and seasonal sets of satellite-based W data using this wind speed exponent. We analyze the deviations of the parametric coefficients a and b from the globally-averaged trend and parameterize these fluctuations explicitly in terms of SST.

3.2.1 Magnitude of regional and seasonal variations

Table 3 exemplifies the results from Eq. (8b): listed are the slopes m and the intercepts c for $W^{1/2}$–U_{10} relationships at 10 and 37 GHz in March 2006 in all 12 regions together with coefficients of determination R^2 and mean U_{10} and T values. Figure 9 visualizes these results by showing examples of the $W^{1/2}$ versus $U_{10QSCAT}$ for different regions and seasons. Figures 9a and 9b show scatter plots for the Gulf of Mexico (region 1) at both frequencies for January 2006. Statistics are presented at the top of the figures and the fit lines are shown in red. Figures 9c and 9d show the fit lines $W^{1/2}(U_{10})$ for 10 and 37 GHz in region 5 for all months, while Figs. 9e and 9f demonstrate variations of the fit lines $W^{1/2}(U_{10})$ for both frequencies over all regions for March 2006.

Deleted: 8

Deleted: s

Deleted: 8

Deleted: 8

Deleted: 8

Deleted: 8

Deleted: 8

Deleted: 8

Figure 9 shows that the variations of the $W^{1/2}(U_{10})$ relationships at 10 GHz are smaller than those for 37 GHz. Focusing on the results for 37 GHz, we note that geographic differences from region to region for a fixed time period (Fig. 9f) yield more variability in the

Deleted: , confirming the same observation reported by SAL13 but obtained with a different analysis

Deleted: 10

$W^{1/2}(U_{10})$ relationship than seasonal variations at a fixed location (Fig. 9d). Because the 37 GHz data provide more information for secondary forcing than the 10 GHz data, the remainder of the data analysis in this study is illustrated with results for W_{37} data. Note that all procedures and analyses described for W_{37} data have been also carried out for the W_{10} data and final results are reported (Sect. 3.3).

Figure 9 also shows that variations of $W^{1/2}$ caused by U_{10} from 3 to 20 m s^{-1} are much larger than the regional and seasonal variations of $W^{1/2}$. While this is expected (because U_{10} is a primary forcing factor), this also points that we need to evaluate whether these regional and seasonal variations are statistically significant. For this, we grouped the values of a and b in two ways: (1) by month with the full range of geographical variability (over all 12 regions) for each month; and (2) by region with the full range of seasonal variability (over all 12 months) for each region. ANOVA test applied to both groups showed that the seasonal variations are not statistically significant, while the regional variations are.

We illustrate this in Fig. 10 with values for b; similar graphs for a show the same results. Figure 10a shows the seasonal cycle for the regionally averaged b values with error bars (± one SD) representing the regional variability. It is clear that the seasonal variations of the regionally averaged b values lay within the regional variability. That is, variations of b from month to month are statistically undistinguishable. Figure 10b illustrates why variations of b from region to region are significantly different. The graph shows the annually averaged b values for each region with error bars representing the seasonal variability. It is clear that the geographical variations are not lost in the seasonal variability.

3.2.2 Quantifying SST variations

The regional differences in Fig. 10b are the variations that we want to quantify with coefficients a and b in terms of secondary factors. The deviations of the regional regression coefficients a and b from the regression coefficients $A = 1\times10^{-4}$ and $B = 1.9$ of the general $W(U_{10})$ dependence (Eq. (11)) give a sense for the magnitude of these variations. The PD between the annually averaged $\langle a\rangle$ and A is about 5% (average for all regions); the average PD between $\langle b\rangle$ and B is 50%. These regional differences can be caused by any or all other secondary factors. It is not trivial to separate (deconvolve) the effects of different factors influencing W data. Because our proxy analysis of the wave field effect produced limited results (Sect. 3.1.1), quantification of the regional differences in terms of wave field is not

Deleted: 10

Deleted: ¶
Figure 9 shows the seasonal cycles of m and c of the $W^{1/2}$ (U_{10}) relationships at 37 GHz in regions 4, 5, 6, and 12. The annual variations of each curve and the variations between the curves confirm the observation from Fig. 8—the variations of m and c over the year are smaller than their variations from region to region. Figure 9 also shows that the seasonal cycles of m and c do not mimic the seasonal cycles of either U_{10} or T (Fig. 3). This implies that m and c are not merely scaling and offsetting the $W^{1/2}$ (U_{10}) relationships, as Eq. (8) suggests, but rather carry more information for the regional and seasonal influences. ¶
As anticipated from Figs. 8a, 8c, and 8e, seasonal cycles for the 10 GHz data reveal much less regional and seasonal influences (not shown).

Deleted: , however,

Deleted: the

Deleted: e.g., s

Deleted: .2

Deleted: s

Deleted: 8 and

Deleted: data

Deleted: for

Deleted: m and c, as well as for

Deleted: ,

Deleted: and H

Deleted: s

Deleted: m, c, and

Deleted: suggests that

Deleted: overall

Deleted: ¶
Note in Fig. 10b that some regional variations might not be distinguished within their seasonal variability. For example, the annual means for regions 1, 4, 7, 8, and 9 all lay within their seasonal variability; likewise, for the annual means for regions 5, 9, and 10. To pinpoint regions with significant differences of b (as well as a, m, and c), we applied the Student test to all possible pairs of regions; e.g., region 1 paired with each region from 2 to 12, region 2 paired with each region from 3 to 12, and so on to a total of 66 pairings of different regions. The Student tests showed statistically different values of b from region to region in 78% of all cases and 58% for a.

Deleted: results of the significantce

Deleted: tests give a rationale for developing the SST dependences $a(T)$ and $b(T)$. Following the data representation

practical. Meanwhile Fig. 3b shows that SST is a distinct characteristic for different regions. This suggests that quantifying the variations of coefficients a and b in terms of SST is a viable possibility. We thus proceed with deriving expressions $a(T)$ and $b(T)$ for the regional variations of the W data; such results are useful to evaluate how well SST can account for the regional variations.

We derived $a(T)$ and $b(T)$ for W data at 37 GHz by relating annually averaged a and b values to the annually averaged T for each region (Fig. 11). Figure 11c shows the monthly means of coefficients b for each region and thus demonstrates how the data points in Fig. 11b have been formed; a similar procedure is used for the data points in Fig. 11a. As in Fig. 10b, the error bars (± one SD) represent the seasonal variability of SST (horizontal bars) and coefficients a and b (vertical bars). A second order polynomial is fitted to the data points in Fig. 11a; a linear fit is applied to the data in Fig. 11b. The correlation coefficients for the derived SST dependences are $R^2 = 0.57$ for $a(T)$ and $R^2 = 0.87$ for $b(T)$. Such R^2 values are consistent with the expectation that SST, being a static secondary factor, affects W more via the offset b than via the slope a.

To evaluate the performance of the quadratic versus cubic wind speed dependence in Eq. (6), we also derived SST dependent coefficients $a(T)$ and $b(T)$ for $n = 3$ following the same procedure as for the case of $n = 2$. We applied Eq. (5b) with $n = 3$ to W_{37} data for all months in regions 4, 5, 6, and 12; we verified that differences due to the use of four instead of twelve regions are not significant. Coefficients a and b were calculated from the m and c values and graphs similar to those in Fig. 11 produced. Linear fits for both a and b were applied to these graphs.

3.3 New parameterization of whitecap fraction

New parameterizations for the whitecap fraction $W(U_{10}, T)$ were obtained from 2006 satellite-based W data by replacing the fixed coefficients in Eqs. (10-11) with SST-dependent coefficients:

$$W = a(T)[U_{10} + b(T)]^2 \quad (13)$$

where

$$a(T) = a_0 + a_1 T + a_2 T^2 \quad (14a)$$

Deleted: w

Deleted: ¶

Deleted: the

Deleted: for

Deleted: the

Deleted: effect

Deleted: using

Deleted: 8

Deleted: the

Deleted: ces

Deleted: 86

Deleted: (Eq. (5b))

Deleted: The absolute values of m and c increase compared to their values obtained with $n = 2$. Specifically, the slopes m in each of the four regions change by 30% to 50%, while their regional variability (i.e., SD) increased by a factor of 3. The y-intercepts c in the four regions become larger than the c values obtained with $n = 2$ by a factor of 4.6, with regional variability increasing by a factor of 2.

However, put together, the fit lines $W^{1/3}(U_{10})$ in region 5 for all months and in all four regions for March 2006 (not shown) behave like those in Figs. 8d and 8f; namely, seasonal variations are smaller than variations from region to region.

Deleted: a

Deleted: are

Deleted: The correlation coefficients for these fits are $R^2 = 0.87$ for $a(T)$ and $R^2 = 0.91$ for $b(T)$.¶
The reason for the different values of m and c (thus a and b) for different n is that each set of coefficients (n, m, c) accounts for primary (i.e., U_{10}) and secondary factors differently. When the expected cubic law is applied to regional data sets which exhibit quadratic wind speed dependences (following from Figs. 5-6), the large differences are reconciled solely by m and c; their values are therefore high. Conversely, smaller values for m and c are required to quantify regional variations when the wind speed exponent is already adjusted to follow the quadratic trend of the data. This confirms the reasoning in Sect. 2.1 that the change from cubic to quadratic wind speed exponent is a major change that the additional parameters impart on the $W(U_{10})$ relationship. The question then is which set of parameters—($n = 2$, m, c) or ($n = 3$, m, c)—better reproduce measured W data. In other words, if the wind speed exponent n is not adjusted but follows the physically determined cubic dependence, can the parametric coefficients m and c alone account for all observed variations of W? We quantify and discuss this point in Sect. 3.3.

Moved down [7]: In other words, if the wind speed exponent n is not adjusted but follows the physically determined cubic dependence, can the parametric coefficients m and c alone account for ...

Deleted: A n

Deleted: as

Deleted: $A = 1\times10^{-4}$ and $B = 1.9$

$$b(T) = b_0 + b_1 T \quad (14b)$$

and the coefficients for data at 10 and 37 GHz are given in Table 4. To evaluate the derived $W(U_{10}, T)$ parameterizations, the whitecap fraction is calculated with Eqs. (13-14) and compared to both parameterized W values and to satellite-based W data.

3.3.1 Comparisons to W parameterizations

The $W(U_{10}, T)$ parameterization for 37 GHz is used here. The W values from SAL13 (37 GHz) and MOM80 are used as references for PD calculations and significance tests (Sect. 2.3). All parameterizations are run for wind speeds from 3 to 20 m s^{-1}.

Figure 12a compares W values from the derived $W(U_{10}, T)$ parameterization at three fixed SST values (T = 2, 12, and 28 °C). Large changes of SST (from 2 to 28 °C) bring relatively small variations between the wind speed trends of W at different T values. The PDs between the three curves are no more than 15%; indeed, significance tests show that the W values at any T remain statistically the same. In addition, W values at any T are not significantly different from the W predictions of the global quadratic $W(U_{10})$ parameterization.

These results qualitatively illustrate the relative contributions of the implicit and explicit accounts for SST effect in the derived parameterization. Namely, large part of the SST and other influences on W is taken care of implicitly by using quadratic wind speed exponent. Much smaller variations are explicitly expressed with the temperature dependent coefficients. Taken together, the set of parametric coefficients—n = 2, $a(T)$, and $b(T)$—accounts for the: (i) full SST effect (i.e., influence on both the trend and the spread of the W data); and (ii) globally-averaged effects of all other secondary factors (i.e., influences only on the trend of W data).

We verify the validity of this deduction by comparing in Fig. 12b W values obtained with the quadratic and cubic $W(U_{10}, T)$ parameterizations at T = 20 °C; MOM80 and SAL13 at 37 GHz are shown for reference. The W values from the cubic $W(U_{10}, T)$ parameterization are not statistically different from those obtained with either the quadratic $W(U_{10}, T)$ or MOM80 for low winds (< 10 m s^{-1}). Different trends of the W values at higher wind speeds suggest that accounting explicitly for SST via $a(T)$ and $b(T)$ in the physically expected cubic wind speed dependence is not sufficient to replicate the satellite-based W data. In other words, when the wind speed exponent n is not adjusted to the data but instead follows the physically

Deleted: ¶
$a_0 = 8.462\times10^{-5}$ ¶
$a_1 = 1.625\times10^{-6}$ ¶
$a_2 = -3.348\times10^{-8}$ . . . . . (14c)¶
$b_0 = 3.354$ ¶
$b_1 = -6.206\times10^{-2}$

Deleted: ¶

Deleted: 10-12 and

Moved down [6]: The W values from SAL13 (37 GHz) and MOM80 are used as references for PD calculations and significance tests (Sect. 2.3).

Moved (insertion) [6]

Deleted: shown here

Moved up [5]: The PD between the global quadratic $W(U_{10})$ and SAL13 at 37 GHz ranges from 0.5% to 10% over the wind speed range. ANOVA and Student tests show that such differences are not statistically significant. That is, the global quadratic $W(U_{10})$ parameterization replicates the trend of the satellite-based W data as well as the SAL13 parameterization, which has a more specific wind speed exponent. Note that we do not expect our $W(U_{10})$ parameterization to be distinctly different ...

Moved down [8]: The PD between the trends ...

Deleted: they seem to fall within each other ...

Deleted: b

Deleted: shows

Deleted: new

Deleted: 8

Deleted: 1

Deleted: ; the parameterizations of SAL13 for 3 ...

Deleted: Physically (from the SST dependence ...

Deleted: 1

Deleted: in

Deleted: ,

Deleted: Applying Student

Deleted: , we find

Deleted: support the anticipated notion (Sect. ...

Deleted: either in $W(U_{10})$ or $W(U_{10}, T)$, we can ...

Deleted: ure

Deleted: c

Deleted: compares

Deleted: With $p > 0.05$ for any fixed T, t

Deleted: Still, the d

Deleted: seen

Deleted: in Fig. 12c

Deleted: That is, when using $n = 3$, one needs t ...

Moved (insertion) [7]

Deleted: values

Deleted: if

determined cubic dependence, explicit representation of the SST effect alone via the parametric coefficients $a(T)$ and $b(T)$ cannot account for all observed variations of W. The implication is that when using cubic wind speed exponent, all secondary factors should be introduced explicitly.

The PD between the trends of the derived $W(U_{10})$ and MOM80 $W(U_{10}, T)$ is from 5% up to 175% with the largest PDs for wind speeds below 7 m s^{-1}. Figure 12 illustrates this with the different trends of the two parameterizations.

3.3.2 Comparisons to *W* data

Here we evaluate how well the derived whitecap fraction parameterizations model the trend and spread of the satellite-based W data. The parameterized W values are calculated using U_{10} and T from the whitecap database (Sect. 2.2.1).

Figure 13a compares W values predicted with both new parameterizations, $W(U_{10})$ and $W(U_{10}, T)$, to the same in situ data plotted in Fig. 1b and to independent satellite-based W data for 10 and 37 GHz from 17 March 2007. Comparisons to the in situ W data demonstrate order-of-magnitude consistency of the W values from the new parameterizations. The new global $W(U_{10})$ parameterizations (black symbols in the Fig. 13a) follows reasonably well the wind speed trends of the satellite-based W data. The W values predicted with the new $W(U_{10}, T)$ parameterization (red and cyan symbols in Fig. 13a) are spread as the satellite-based W data. The cluster of W values predicted with $W(U_{10}, T)$ are statistically different from the MOM80 $W(U_{10})$ parameterizations. This is the most important result of this study: we demonstrate that accounting for at least one secondary factor, we are able to model both the trend and the spread of the W values.

Note in Fig. 13a that the new $W(U_{10}, T)$ parameterization does not predict the spread of the satellite-based W data entirely. This suggests that accounting explicitly for SST in a W parameterization is not enough to replicate all the natural variability (spread) of W. This is consistent with our general understanding of the need to explicitly include many secondary factors in W parameterizations, not just SST (Sect. 2.1).

Though SST entails small variations in the trend of W with U_{10} (Figs. 12a and 13a), important consequence of the newly derived $W(U_{10}, T)$ parameterization is that it shapes significantly different spatial distribution compared to cubic and higher wind speed dependences like that of the MOM80. Figure 13b shows a difference map between the global

Deleted: can
Deleted: *m*
Deleted: *c*
Deleted: alone
Deleted: ?
Moved (insertion) [8]
Deleted: global quadratic
Deleted: Though
Deleted: a
Deleted: shows visibly
Deleted: from both
Moved down [9]: Comparisons to the published in situ *W* data demonstrate order-of-magnitude consistency of the *W* values from the new parameterizations.
Deleted: Because there are no other remotely-sensed *W* data except those from WindSat, the most we can do at the moment is to evaluate how well the new parameterizations can replicate the trend and the spread of the satellite-based *W*. Recently, *W* values from a global wave model were compared to *W* from MOM80 and WindSat by Leckler et al. (2013), so one can evaluate where modeled *W* values stand in the comparison of data and parameterizations of *W*. All
Deleted: shown here
Deleted: , i.e., U_{10} from QuikSCAT and *T* from GDAS
Deleted: plotted in Fig. 1b; comparisons to ...
Moved (insertion) [9]
Deleted: published
Deleted: quadratic
Deleted: f
Deleted: ure
Deleted: closely
Deleted: This lends confidence in the use of the ...
Deleted: represent
Deleted: the
Deleted: of
Deleted: fairly well; tests show that they do no ...
Deleted: , however,
Deleted: both the new quadratic and
Deleted: when we model only the trend of *W* w ...
Deleted: , the result is a significant difference w ...
Deleted: I
Deleted: , one can notice
Deleted: b
Deleted: the most
Deleted: quadratic
Deleted: The complex behavior seen in Fig. 12l ...

annual average W distributions for 2006. The MOM80 relationship yields a wider W range with higher values in regions with the highest wind speeds. In particular, this occurs between about 40° and 70° in the Southern ocean and in the North Atlantic. The latitudinal variations from the Equator to the poles are more pronounced when using the MOM80 relationship as compared to Eqs. (13-14). The new $W(U_{10}, T)$ parameterization provides a global spatial distribution with similar patterns, but the absolute values are lower at high latitudes and higher at low latitudes. Note that in most studies, as in this study, $W(U_{10})$ of MOM80 is extrapolated beyond the range of the data from which it was derived (Sect. 1). This could be a reason for the large differences between the two parameterizations at higher wind speeds (and especially in cold waters).

3.4 Sea spray aerosol production

The newly derived $W(U_{10}, T)$ parameterization (Eqs. (13-14)) was used to estimate the global annual average emission of super-micron SSA using M86 SSSF (Eq. (4′)). The total (i.e., size integrated) annual SSA mass emission for 2006 is 4359.69 Tg yr^{-1} (4.4×10^{12} kg yr^{-1}). This is about 50% larger than that calculated with the M86 SSSF using MOM80 (Eq. (4)), 2915 Tg yr^{-1} (2.9×10^{12} kg yr^{-1}). Because we have shown that the new $W(U_{10}, T)$ and MOM80 $W(U_{10})$ are significantly different (Sect. 3.3.2), we infer that the SSA emissions based on SSSFs using each parameterization in combination with the same shape factor (Eq. (4′)) also differ significantly. The two estimates of SSA emissions are calculated using the same modelling tool (Sect. 2.4) and the same input data (Sect. 2.2.1). Keeping everything the same but the magnitude factor guarantees that the 50% difference is due solely to the account for the SST effect on W. The spatial distribution of the mass emission rates obtained with SSSFs using the new $W(U_{10}, T)$ is shown in Fig. 14a. The SSA emissions obtained with the new and the MOM80 $W(U_{10})$ parameterizations mimic the patterns of the W distributions. The differences are mapped in Fig. 14b.

Previously modeled total dry SSA mass emissions vary by two orders of magnitude because of a variety of uncertainty sources (Sect. 1): $(2.2–22)\times10^{12}$ kg yr^{-1} (Textor et al., 2006, their Fig. 1a; de Leeuw et al., 2011, their Table 1); and $(2–74)\times10^{12}$ kg yr^{-1} for long-term averages (over 25 years) (G14, their Table 2, excluding 3 outliers). The impact of the modeling method used has to be acknowledged too. Grythe et al. (2014) suggest that the spread in published estimates of global emission based on the same M86 SSSF (Eq. (4)), from

Deleted: erefore,

Deleted:), the W values that are obtained using the MOM80 parameterization are somewhat questionable

Moved up [4]: At the same time, the QuikSCAT instrument, which provided the U_{10} satellite data used in this study, has a decreased sensitivity for wind speeds over 20 m s^{-1} (Quilfen et al., 2007). All results regarding higher wind speeds should, therefore, be handled with caution.

Deleted: At the same time, the QuikSCAT instrument, which provided the U_{10} satellite data used in this study, has a decreased sensitivity for wind speeds over 20 m s^{-1} (Quilfen et al., 2007). All results regarding higher wind speeds should, therefore, be handled with caution. Only continuo ...

Deleted: quadratic

Deleted: quadratic

Deleted: these two

Deleted: s

Deleted: with

Deleted: Without any change in the shape factor

Deleted: , this

Deleted: explicit

Deleted: ing

Deleted: ¶

3.3×10^{12} to 11.7×10^{12} kg yr^{-1} (Lewis and Schwartz, 2004), can be attributed to differences in model input data and resolution differences. An example of the same SSSF yielding different results when applied in different models is also seen in the work of de Leeuw et al. (2011, their Table 1).

For a meaningful comparison of our results to SSA emissions obtained with other SSSFs, we attempt to remove (or at least minimize) the impact of the modeling method. As in this study, G14 used the same model (i.e., input data and configuration) to evaluate 21 SSSFs, including that of M86, against measurements. We thus can infer a "modelling" factor using our and G14 results obtained with M86 SSSF. We find that the G14 estimate of SSA emission from M86 (4.51×10^{12} kg yr^{-1}) is 1.55 times larger than our estimate of 2.9×10^{12} kg yr^{-1} from M86 and MOM80. We apply this factor of 1.55 to our SSA emission estimated with the new $W(U_{10}, T)$ parameterization and obtain a "model scaled" value of 6.75×10^{12} kg yr^{-1}. Our "model scaled" estimate of the SSA emission is close to the median 5.91×10^{12} kg yr^{-1} of the SSA emissions reported by G14. This shows that an SSSF with a magnitude factor derived from satellite-based W data provides reasonable and realistic predictions of the SSA emission.

To narrow down this broad assessment, we now look at the SSSFs evaluated by G14 which account for the SST effect on SSA emissions. There are four such SSSFs in the G14 study (see their Table 2): S11T of Sofiev et al. (2011), G03T of Gong (2003), J11T of Jaeglé et al. (2011), and G13T of G14. To minimize differences caused by using different size ranges, we focus on S11T and G13T, both applied to dry SSA diameters $D_p = r_{80}$ (Sect. 2.4) from 0.01 to 10 μm. The upper limit is the same as in our study, while the lower limit is extended to sub-micron sizes, which, as we have seen (Sect. 2.4.2), introduces a discrepancy of about 14%.

The original Sofiev et al. (2011) SSSF is based on the M86 SSSF (Eq. (4)) combined with data from laboratory experiments by Mårtensson et al. (2003) to account for SST and salinity effects and a field experiment by Clarke et al. (2006) to extend the size range. In the G14 study, the salinity weight proposed by Sofiev et al. (2011) is not applied. At a reference salinity of 33 ‰, S11T estimates an SSA emission of 2.59×10^{12} kg yr^{-1}. Without the SST effect (the SST factor set to unity), the SSA emission estimated with S11 is 5.87×10^{12} kg yr^{-1}. With everything else the same except for the SST factor in source functions S11 and S11T, we evaluate that accounting for the SST effect results in changes by 56%. Correcting for 14%

discrepancy due to extended lower size limit, we infer a 42% change when the SST effect is included in the SSSF. This is comparable to the 50% change due to SST in our case. We surmise that parameterizing additional influences on W is a viable way to account and explain some of the uncertainty of SSA emissions.

Grythe et al. (2014) used a large data set of ship observations to develop G13T by changing both the magnitude and the shape factors. The authors modified the SSSF of Smith and Harrison (1998) (a sum of two log-normal distributions) to add an extra log-normal mode to cover the accumulation mode. They also added the empirically based SST factor (a third order polynomial) proposed by Jaeglé et al. (2011). With G13T, G14 estimate an SSA emission of 8.91×10^{12} kg yr^{-1}. The functional forms of the magnitude (involving the SST effect) and shape (modelling the size distribution) factors of G13T and S11T are very different. This makes it difficult to evaluate the relative contribution of the magnitude and shape factors for variations in SSA emissions. Our results can help.

The shape factors of S11T and our SSSF using $W(U_{10}, T)$ have a similar (not identical) functional form (that of M86, original and modified), but the functional forms accounting for SST are different. Our SSA emission estimate is about 62% higher than that of S11T. Allowing for 14% discrepancy due to the lower size limit, we find that different approaches to account for SST lead to about 67% variation in SSA emissions. Compared to G13T, our SSSF using $W(U_{10}, T)$ has a different shape factor (that of M86 versus log-normal), and a similar (but not identical) functional form for the SST effect (polynomial). Our SSA emission estimate is about 32% lower than that of G13T. Allowing for 14% size discrepancy, we find that different shape factors lead to about 13% variation in SSA emissions.

On the basis of these assessments, we can state that the inclusion of the SST effect in the magnitude factor and/or the choice of the shape factor (size range and model for the size distribution) in the SSSF can explain 13%-67% of the variations in the predictions of SSA emissions. The spread in SSA emission can thus be constrained by more than 100% when improvements of both the magnitude and the shape factor are pursued. Our results on the W parameterization (Fig. 13a) suggest that accounting for more secondary forcing in the magnitude factor would explain more fully the spread among SSA emissions.

Moved up [2]: Because, after wind speed, the most important secondary factor that accounts for variability in W is the wave field (SAL13), efforts to include wave parameters in W parameterizations are well justified.

4 Conclusions

The objective of the study presented here is to evaluate how accounting for natural variability of whitecaps in the parameterization of the whitecap fraction W would affect mass flux predictions when using a sea spray source function based on the discrete whitecap method. The study uses satellite-based W data estimated from measurements of the ocean surface brightness temperature T_B by satellite-borne microwave radiometers at frequencies of 10 and 37 GHz, W_{10} and W_{37}. Global and regional data sets comprising W_{10} and W_{37} data, wind speed U_{10}, and sea surface temperature T for 2006 were used to derive parameterizations $W(U_{10})$ and $W(U_{10}, T)$. The SSSF of Monahan et al. (1986) combined with the new $W(U_{10}, T)$ was used to estimate sea spray aerosol emission. The conclusions of the study are the following.

Assessment of the global W data set revealed a quadratic correlation between W and U_{10} (Eqs. (10-11) and Sect. 3.1.1). The unconventional positive y-intercept for $W_{37}(U_{10})$ could be interpreted as a mathematical expression of the static forcing that given seawater properties (e.g., effects of SST, salinity, and surfactant concentrations) impart on whitecaps. Parameterization $W(U_{10})$ derived with an independent data set (U_{10} from ECMWF instead of QuikSCAT) helps to determine that the intrinsic correlation between W and U_{10} is most likely less than about 4% (Sect. 3.1.2). Proxy analysis of satellite-based W data at increasing and decreasing wind speeds yields limited results for the effect of the wave field on W (Sect. 3.1.1). The derived $W(U_{10})$ for both W_{10} and W_{37} replicate the trend of the satellite-based data well (Fig. 13a). That is, the adjusted quadratic wind speed exponent in $W(U_{10})$ accounts implicitly for most of the SST variations. The new quadratic $W(U_{10})$ predicts whitecap fraction significantly different from that obtained with the widely used $W(U_{10})$ of MOM80.

Applying the global $W(U_{10})$ parameterization on regional scale shows that the seasonal variations of its regression coefficients a and b are not statistically significant, while the regional variations are. On this basis, by relating annually averaged a and b values to the annually averaged T for each region (Fig. 11), the explicit SST dependences $a(T)$ and $b(T)$ for data at 10 and 37 GHz were derived (Sect. 3.3. and Table 4). The new $W(U_{10}, T)$ parameterization (Eqs. (13-14)) is able to model the variability (spread) of the satellite-based W data (Fig. 13a). The capability of the new $W(U_{10}, T)$ parameterization to model both the trend and the spread of the W data sets it apart from all other $W(U_{10})$ parameterizations (e.g., MOM80 and SAL13). Results show that besides SST, one needs to include explicitly other secondary factors in order to model the full spread of the satellite-based W. Including the SST

Deleted: ¶

Deleted: only at extreme conditions (high winds and cold waters)

Deleted: quadratic

Deleted: quadratic

Deleted: predicts small variations in the trend of W for different SST values (Fig. 12b). However, when used with real U_{10} and T data, the new $W(U_{10}, T)$ parameterization replicates

Deleted: well

effect via $a(T)$ and $b(T)$ in the physically expected cubic wind speed dependence is not sufficient to replicate the trend of the satellite-based W values. While SAL13 analysis of the satellite-based whitecap database demonstrated the influences of secondary factors on whitecap fraction, our study goes a step further in using the satellite-based W data to parameterize one of these influences, that of SST.

Application of the new $W(U_{10}, T)$ parameterization in the Monahan et al. (1986) SSSF resulted in a total (integrated only over super-micron sizes) SSA mass emission estimate of 4359.69 Tg yr^{-1} (4.4×10^{12} kg yr^{-1}) for 2006. Scaled for modeling differences (Sect. 3.4), this estimate is 6.75×10^{12} kg yr^{-1}, which is comparable to previously reported estimates. Comparing our and previous total SSA emissions, we have been able to assess to what degree accounting for the SST influence on whitecaps can explain the spread of SSA emissions. With or without the SST effect included in the SSSF, SSA emissions obtained with the new $W(U_{10}, T)$ parameterization vary by ~50%. Different approaches to account for SST effect yield ~67% variations. Different models for the size distribution applied to different size ranges lead to 13%-42% variations in SSA emissions. Understanding and constraining the various sources of uncertainty in the SSSF would eventually improve the accuracy of SSSF predictions. Including the natural variability of whitecaps in the SSSF magnitude factor is a viable way toward such accuracy improvement.

Deleted: quadratic

While the new $W(U_{10}, T)$ parameterization is able to model the trend and the spread of the satellite-based W data, the SST variations are relatively small. To model the full variability of W, future work should focus on the parameterization of the wave field effect. The extended version of the whitecap database contains wave field characteristics and is thus suitable for such quantification. It is recommended that the extended whitecap database includes wind speed data from independent source(s) matched in time and space at WindSat resolution.

Data availability

The data analysis and the results reported in this study are available from the corresponding author M.F.M.A. (Monique) Albert (monique.albert@tno.nl).

Acknowledgements

This study is partly funded by SRON, Netherlands Institute for Space Research, through the Dutch Users Support Programme GO-2. MDA was sponsored by the Office of Naval

Research, NRL Program element 61153N, WU 4500. GdL by was supported by the European Space Agency (Support to Science Element: Oceanflux Sea Spray Aerosol, contract No. 4000104514/11/I-AM), the Centre on Excellence in Atmospheric Science funded by the Finnish Academy of Sciences Excellence (project no. 272041), the CRAICC project (part of the Top-level Research Initiative).

References

Albert, M. F. M. A., Schaap, M., de Leeuw, G., and Builtjes, P. J. H.: Progress in the determination of the sea spray source function using satellite data, Journal of Integrative Environmental Sciences, 7, 159-166, 2010.

Albert, M. F. M. A., Schaap, M., Manders, A. M. M., Scannell, C., O'Dowd, C. D., and de Leeuw, G.: Uncertainties in the determination of global sub-micron marine organic matter emissions, Atmos. Environ., 57, 289-300, 2012.

Andreae, M. O. and Crutzen, P. J.: Atmospheric aerosols: biogeochemical sources and role in atmospheric chemistry, Science, 276, 1052-1058, 1997.

Andreas, E. L.: Sea Spray and the turbulent air-sea heat fluxes, J. Geophys. Res., 97, 11429-11441, 1992.

Anguelova, M. D: Assessing the utility of satellite-based whitecap fraction to estimate sea spray production and CO2 transfer velocity, IOP Conf. Ser.: Earth Environ. Sci., 35, 012002, 2016.

Anguelova, M. D. and Gaiser, P. W.: Skin depth at microwave frequencies of sea foam layers with vertical profile of void fraction, J. Geophys. Res., 116, C11002, 2011.

Anguelova, M. D. and Gaiser, P. W.: Microwave emissivity of sea foam layers with vertically inhomogeneous dielectric properties, Remote Sens. Environ., 139, 81-96, 2013.

Anguelova, M. D. and Webster, F.: Whitecap coverage from satellite measurements: A first step toward modeling the variability of oceanic whitecaps. J. Geophys. Res., 111, C03017, 2006.

Anguelova, M. D., Bettenhausen, M. H., and Gaiser, P. W.: Passive remote sensing of sea foam using physically-based models, in: Proceedings of the IGARSS 2006: IEEE International Geoscience and Remote Sensing Symposium, Denver, Colorado, USA, 31 July-4 August, 3659-3662, 2006.

Anguelova, M. D., Bettenhausen, M. H., Johnston, W. F., Gaiser, P. W.: First extensive whitecap database and its use to study whitecap fraction variability, in: Proceedings of the 17th Air-Sea Interaction Conference, AMS, Annapolis, Maryland, USA, 26 - 30 September, 2010 (http://ams.confex.com/ams/pdfpapers/174036.pdf).

Anguelova, M. D., Bobak, J. P., Asher, W. E., Dowgiallo, D. J., Moat, B. I., Pascal, R. W., and Yelland, M. J.: Validation of satellite-based estimates of whitecap coverage: approaches and initial results, in: Proceedings of the 16th Air-Sea Interaction conference, AMS, Phoenix, Arizona, USA, 10-15 January, 2009, (http://ams.confex.com/ams/pdfpapers/143665.pdf).

Asher, W. E. and Wanninkhof, R.: The effect of bubble-mediated gas transfer on purposeful dual-gaseous tracer experiments, J. Geophys. Res., 103, 10,555-10,560, 1998.

Barrie, L. A., Bottenheim, J. W., Schnell, R. C., Crutzen, P. J., and Rasmussen, R. A.: Ozone destruction and photochemical reactions at polar sunrise in the lower Arctic atmosphere, Nature, 334, 138–141, 1988.

Bettenhausen, M. H., Smith, C. K., Bevilacqua, R. M., Wang, N. –Y., Gaiser, P. W., and Cox, S.: A nonlinear optimization algorithm for WindSat wind vector retrievals, IEEE T. Geosci. Remote, 44, 597-610, 2006.

Blanchard, D. C.: The electrification of the atmosphere by particles from bubbles in the sea, Prog. Oceanogr., 1, 73-112, 1963.

Blanchard, D. C.: The production, distribution, and bacterial enrichment of the sea-salt aerosol, in: Air-sea exchange of gases and particles, Liss, P. S. and Slinn, W. G. N., D. Reidel Publishing Company, Dordrecht, The Netherlands, 407-454, 1983.

Bondur, V., and Sharkov, E.: Statistical properties of whitecaps on a rough sea, Oceanology, 22, 274– 279, 1982.

Callaghan, A. H.: An improved whitecap timescale for sea spray aerosol production flux modeling using the discrete whitecap method, J. Geophys. Res.-Atmos., 118, 9997-10010, 2013.

Callaghan, A. H. and White, M.: Automated processing of sea surface images for the determination of whitecap coverage, J. Atmos. Ocean. Tech., 26, 383-394, 2009.

Callaghan, A. H., de Leeuw, G., Cohen, L., and O'Dowd, C. D.: Relationship of oceanic whitecap coverage to wind speed and wind history, Geophys. Res. Lett., 35, L23609, 2008.

Callaghan, A. H., Deane, G. B., and Stokes, M. D.: Two Regimes of Laboratory Whitecap Foam Decay: Bubble-Plume Controlled and Surfactant Stabilized, J. Phys. Oceanogr., 43, 1114-1126, 2013.

Chameides, W. L. and Stelson, A. W.: Aqueous-phase chemical processes in deliquescent sea-salt aerosols: a mechanism that couples the atmospheric cycles of S and sea salt, J. Geophys. Res.- Atmos., 97, 20565-20580, 1992.

Chelton, D. B. and Freilich, M. H.: Scatterometer-based assessment of 10-m wind analyses from the operational ECMWF and NCEP numerical weather prediction models, Mon. Weather Rev., 133, 409-429, 2005.

Cicerone, R. J.: Halogens in the atmosphere, Rev. Geophys. Space Ge., 19 (NO. 1), 123-139, 1981.

Clarke, A. D., Owens, S. R., and Zhou, J.: An ultrafine sea-salt flux from breaking waves: Implications for cloud condensation nuclei in the remote marine atmosphere, J. Geophys. Res., 111, D06202, 2006.

de Leeuw, G., Andreas, E. L., Anguelova, M. D., Fairall, C. W., Lewis, E. R., O'Dowd, C. D., Schulz, M., and Schwartz, S. E.: Production flux of sea-spray aerosol, Rev. Geophys., 49, RG2001, 2011.

Facchini, M. C., Rinaldi, M., Decesari, S., Carbone, C., Finessi, E., Mircea, M., Fuzzi, S., Ceburnis, D., Flanagan, R., Nilsson, E. D., de Leeuw, G., Martino, M., Woeltjen, J., and O'Dowd, C. D.: Primary submicron marine aerosol dominated by insoluble organic colloids and aggregates, Geophys. Res. Lett., 35, L17814, 2008.

Fairall, C. W., Kepert, J. D., and Holland, G. J.: The effect of sea spray on surface energy transports over the ocean, The Global Atmosphere and Ocean System, 2, 121-142, 1994.

Falkowski, P. G., Barber, R. T., and Smetacek, V.: Biogeochemical controls and feedbacks on ocean primary production, Science, 281, 200-206, 1998.

Ghan, S. J., Guzman, G., and Hayder, A. -R.: Competition between sea salt and Sulfate particles as cloud condensation nuclei, J. Atmos. Sci., 55, 3340-3347, 1998.

Gaiser, P.W., St. Germain, K. M., Twarog, E. M., Poe, G. A., Purdy, W., Richardson, D., Grossman, W., Linwood Jones, W., Spencer D., Golba, G., Cleveland, J., Choy, L., Bevilacqua, R. M., and Chang, P. S.: The WindSat spaceborne polarimetric microwave radiometer: sensor description and early orbit performance, IEEE T. Geosci. Remote, 42, NO. 11, 2347–2361, 2004.

Garrett, W. D.: Stabilization of air bubbles at the air-sea interface by surface-active material, Deep-Sea Res., 14, 661-672, 1967.

Goddijn-Murphy, L., Woolf, D. K., and Callaghan, A. H.: Parameterizations and algorithms for oceanic whitecap coverage, J. Phys. Oceanogr., 41, 742-756, 2011.

Gong, S. L.: A parameterization of sea-salt aerosol source function for sub- and super-micron particles, Global Biogeochem. Cycles, 17, 1097, 2003.

Graedel, T. E. and Keene, W. C.: The budget and cycle of Earth's natural chlorine, Pure Appl. Chem., 68, 1689-1697, 1996.

Grythe, H., Ström, J., Krejci, R., Quinn, P., and Stohl, A.: A review of sea-spray aerosol source functions using a large global set of sea salt aerosol concentration measurements, Atmos. Chem. Phys., 14, 1277–1297, 2014.

Hanson, J. L., and Phillips, O. M.: Wind sea growth and dissipation in the open ocean, J. Phys. Oceanogr., 29, 1633-1648, 1999.

Jaeglé, L., Quinn, P. K., Bates, T. S., Alexander, B., and Lin, J.-T.: Global distribution of sea salt aerosols: new constraints from in situ and remote sensing observations, Atmos. Chem. Phys., 11, 3137-3157, doi:10.5194/acp-11-3137-2011, 2011.

Kara, A. B., Wallcraft, A. J., and Bourassa, M. A.: Air-sea stability effects on the 10 m winds over the global ocean: Evaluations of air-sea flux algorithms, J. Geophys. Res.-Oceans, 113, C04009, 2008.

Keene, W. C., Pszenny, A. A. P., Jacob, D. J., Duce, R. A., Galloway, J. N., Schultz-Tokos, J. J., Sievering, H., and Boatman, J. F.: The geochemical cycling of reactive chlorine through the marine troposphere, Global Biogeochem. Cy., 4 (NO. 4), 407-430, 1990.

Keene, W. C., Khalil, M. A. K., Erickson, D. J., McCulloch, A., Graedel, T. E., Lobert, J. M., Aucott, M. L., Gong, S.-L., Harper, D. B., Kleiman, G., Midgley, P., Moore, R. M., Seuzaret, C., Sturges, W. T., Benkovitz, C. M., Koropalov, V., Barrie, L. A., and Li, Y.-F.: Composite global emissions of reactive chlorine from anthropogenic and natural sources: reactive chlorine emissions inventory, J. Geophys. Res., 104 (NO. D7), 8429-8440, 1999.

Kleiss, J. M. and Melville, W. K.: The analysis of sea surface imagery for whitecap kinematics, J. Atmos. Ocean. Tech, 28, 219-243, 2011.

Koop, T., Kapilashrami, A., Molina, L.T., and Molina, M. J.: Phase transitions of sea-salt/water mixtures at low temperatures: implications for ozone chemistry in the polar marine boundary layer, J. Geophys. Res., 105 (NO. D21), 26393-26402, 2000.

Lewis, E. R. and Schwartz, S. E.: Sea salt aerosol production: mechanisms, methods, measurements and models - A critical review, Geoph. Monog. Series, 152, American Geophysical Union, Washington D. C., 413 pp, 2004.

Luria, M. and Sievering, H.: Heterogeneous and homogeneous oxidation of SO_2 in the remote marine atmosphere, Atmos. Environ., 25A, 1489-1496, 1991.

Mårtensson, E. M., Nilsson, E. D., de Leeuw, G., Cohen, L. H., and Hansson, H.–C.: Laboratory simulations and parameterization of the primary marine aerosol production, J. Geophys. Res., 108, 4297, 2003.

Medwin, H.: In situ acoustic measurements of microbubbles at sea, J. Geophys. Res., 82, 971-976, 1977.

Meissner, T. and Wentz, F. J.: The emissivity of the ocean surface between 6 and 90 GHz over a large range of wind speeds and earth incidence angles, IEEE T. Geosci. Remote, 50, 3004-3026, 2012.

Melville, W. K.: The role of surface-wave breaking in air-sea interaction, Annu. Rev. Fluid Mech., 28, 279-321, 1996.

Monahan, E. C.: Oceanic Whitecaps, J. Phys. Oceanogr., 1, 139-144, 1971.

Monahan, E. C. and O'Muircheartaigh, I.: Optimal power-law description of oceanic whitecap coverage dependence on wind speed, J. Phys. Oceanogr., 10, 2094–2099, 1980.

Monahan, E. C. and O'Muircheartaigh, I.: Whitecaps and the passive remote sensing of the ocean surface, Int. J. Remote Sens., 7, 627-642, 1986.

Monahan, E. C. and Woolf, D. K.: Comments on "Variations of whitecap coverage with wind stress and water temperature, J. Phys. Oceanogr., 19, 706–709, 1989.

Monahan, E. C., Fairall, C. W., Davidson, K. L., and Boyle, P. J.: Observed inter-relations between 10 m winds, ocean whitecaps and marine aerosols, Q. J. Roy. Meteor. Soc., 109, 379-392, 1983.

Deleted: Leckler, F., Arduin, F., Filipot, J.-F., Mironov, A.: Dissipation source terms and whitecap statistics, Ocean Modell., 70, 62-74, 2013. ¶

Monahan, E. C., Spiel, D. E., and Davidson, K. L.: A model of marine aerosol generation via whitecaps and wave disruption, in: Oceanic whitecaps: and their role in air-sea exchange processes, Monahan, E. C., Mac Niocaill, G., D. Reidel Publishing Company, Dordrecht, The Netherlands, 167-174, 1986.

Norris, S. J., Brooks, I. M., Moat, B. I., Yelland, M. J., de Leeuw, G., Pascal, R. W., Brooks, B. J.: Near-surface measurements of sea spray aerosol production over whitecaps in the open ocean. Ocean Science, 9, 133–145, doi: 10.5194/os-9-133-2013, 2013a.

Norris, S. J., Brooks, I. M., and Salisbury, D. J.: A wave roughness Reynolds number parameterization of the sea spray source flux, Geophys. Res. Lett., 40, 4415–4419, 2013b.

O'Dowd, C. D. and de Leeuw, G.: Marine aerosol production: a review of the current knowledge, Philos. T. R. Soc. A, 365, 1753-1774, 2007.

O'Dowd, C. D., Lowe, J. A., Smith, M. H., and Kaye, A. D.: The relative importance of non-sea-salt sulphate and sea-salt aerosol to the marine cloud condensation nuclei population: An improved multi-component aerosol-cloud droplet parametrization, Q. J. Roy. Meteor. Soc., 125, 1295-1313, 1999.

O'Dowd, C. D., Facchini, M. C., Cavalli, F., Ceburnis, D., Mircea, M., Decesari, S., Fuzzi, S., Yoon, Y. J., and Putaud, J.-P.: Biogenically driven organic contribution to marine aerosol, Nature, 431, 676-680, 2004.

Ovadnevaite, J., Manders, A., de Leeuw, G., Ceburnis, D., Monahan, C., Partanen, A .-I., Korhonen, H., and O'Dowd, C. D.: A sea spray aerosol flux parameterization encapsulating wave state, Atmos. Chem. Phys., 14, 1837-1852, 2014.

Paget, A. C., Bourassa, M. A., and Anguelova, M. D.: Comparing in situ and satellite-based parameterizations of oceanic whitecaps, J. Geophys. Res. Oceans, 120, 2826–2843, 2015.

Pandey, P. C. and Kakar, R. K.: An empirical microwave emissivity model for a foam-covered sea, IEEE J. Oceanic Eng., 7, 135-140, 1982.

Partanen, A.-I., Dunne, E. M., Bergman, T., Laakso, A., Kokkola, H., Ovadnevaite, J., Sogacheva, L., Baisnée, D., Sciare, J., Manders, A., O'Dowd, C., de Leeuw, G., and Korhonen, H.: Global modelling of direct and indirect effects of sea spray aerosol using a source function encapsulating wave state, Atmos. Chem. Phys., 14, 11731-11752, 2014.

Quilfen, Y., Prigent, C., Chapron, B., Mouche, A. A., and Houti, N.: The potential of QuikSCAT and WindSat observations for the estimation of sea surface wind vector under severe weather conditions, J. Geophys. Res., 112, C09023, 2007.

Reising, S., Asher, W., Rose, L., and Aziz, M.: Passive polarimetric remote sensing of the ocean surface: The effects of surface roughness and whitecaps, paper presented at the International Union of Radio Science, URSI Gen. Assem., Maastrict, Netherlands, 2002.

Saiz-Lopez, A. and von Glasow, R.: Reactive halogen chemistry in the troposphere, Chem. Soc. Rev., 41, 6448-6472, 2012.

Salisbury, D. J., Anguelova, M. D., and Brooks, I. M.: On the variability of whitecap fraction using satellite-based observations, J. Geophys. Res.-Oceans, 118, 6201-6222, 2013.

Salisbury, D. J., Anguelova, M. D., and Brooks, I. M.: Global distribution and seasonal dependence of satellite-based whitecap fraction, Geophys. Res. Lett., 41, 1616–1623, 2014.

Savelyev, I. B., Anguelova, M. D., Frick, G. M., Dowgiallo, D. J., Hwang, P. A., Caffrey, P. F., and Bobak, J. P.: On direct passive microwave remote sensing of sea spray aerosol production, Atmos. Chem. Phys., 14, 11611-11631, 2014.

Sievering, H., Boatman, J., Gorman, E., Kim, Y., Anderson, L., Ennis, G., Luria, M., and Pandis, S.: Removal of sulphur from the marine boundary layer by ozone oxidation in sea-salt aerosols, Nature, 360, 571-573, 1992.

Sievering, H., Gorman, E., Ley, T., Pszenny, A., Springer-Young, M., Boatman, J., Kim, Y., Nagamoto, C., and Wellman, D.: Ozone oxidation of sulfur in sea-salt aerosol particles during the Azores Marine Aerosol and Gas Exchange experiment, J. Geophys. Res. -Atmos., 100, 23075-23081, 1995.

Smith, M. H., Park, P. M., and Consterdine, I. E.: Marine aerosol concentrations and estimated fluxes over the sea, Q. J. Roy. Meteor. Soc., 119, 809–824, 1993.

Smith, M. H. and Harrison, N. M.: The sea spray generation function, J. Aerosol Sci., 29 (Suppl. 1), S189-S190, 1998.

Sofiev, M., Soares, J., Prank, M., de Leeuw, G., and Kukkonen, J.: A regional-to-global model of emission and transport of sea salt particles in the atmosphere, J. Geophys. Res., 116, D21302, 2011.

Stramska, M. and Petelski, T.: Observations of oceanic whitecaps in the north polar waters of the Atlantic, J. Geophys. Res., 108, NO. C3, 3086, 2003.

Tang, W., Yueh, S. H., Fore, A. G., and Hayashi A.: Validation of Aquarius sea surface salinity with in situ measurements from Argo floats and moored buoys, J. Geophys. Res. Oceans, 119, 6171–6189, 2014, doi:10.1002/2014JC010101.

Textor, C., Schulz, M., Guibert, S., Kinne, S., Balkanski, Y., Bauer, S., Berntsen, T., Berglen, T., Boucher, O., Chin, M., Dentener, F., Diehl, T., Easter, R., Feichter, H., Fillmore, D., Ghan, S., Ginoux, P., Gong, S., Grini, A., Hendricks, J., Horowitz, L., Huang, P., Isaksen, I., Iversen, T., Kloster, S., Koch, D., Kirkevåg, A., Kristjansson, J. E., Krol, M., Lauer, A., Lamarque, J. F., Liu, X., Montanaro, V., Myhre, G., Penner, J., Pitari, G., Reddy, S., Seland, Ø., Stier, P., Takemura, T., and Tie, X.: Analysis and quantification of the diversities of aerosol life cycles within AeroCom, Atmos. Chem. Phys., 6, 1777-1813, 2006.

Toba, Y. and Chaen, M.: Quantitative expression of the breaking of wind waves on the sea surface, Records of Oceanographic Works in Japan, 12 (NO. 1), 1-11, 1973.

Thorpe, S. A.: On the clouds of bubbles formed by breaking wind-waves in deep water, and their role in air-sea gas transfer, Philos. T. R. Soc. S. -A., 304, 155-210, 1982.

Wanninkhof, R., Asher, W. E., Ho, D. T., Sweeney, C., and McGillis, W. R.: Advances in quantifying air-sea gas exchange and environmental forcing, Annual Review of Marine Science, 1, 213-244, 2009.

Wentz, F. J.: A model function for ocean microwave brightness temperatures, J. Geophys. Res., 88, NO. C3, 1892-1908, 1983.

Wentz, F. J.: A well-calibrated ocean algorithm for special sensor microwave / imager, J. Geophys. Res., 102, NO. C4, 8703-8718, 1997.

Woolf, D. K.: Bubbles and their role in gas exchange, in: The Sea Surface and Global Change, Liss, P. S. and Duce, R. A., Cambridge Univ. Press, New York, 173-205, 1997.

Wu, J.: Variations of whitecap coverage with wind stress and water temperature, J. Phys. Oceanogr., 18, 1448-1453, 1988.

Zhao, D. and Toba, Y.: Dependence of whitecap coverage on wind and wind-wave properties, J. Oceanogr., 57, 603-616, 2001.

Table 1

Coordinates, number of data points, range and mean value for wind speed, and range and mean value of SST of selected regions (a) for January 2006, (b) for July 2006.

a

Region	Lon.	Lat.	Number of samples*	Wind speed* [m s^{-1}]			SST* [°C]		
				Range	Mean	Median	Range	Mean	Median
1.	86°W − 95°W	23°N–28°N	18896	1.3−15.7	7.5	7.6	19.4−26.0	23.8	24.1
2.	1°W − 15°W	1°S – 30°S	169128	0.2−12.9	6.4	6.4	21.4−27.8	24.2	24.1
3.	75° E − 89° E	1°S −30°S	169056	0.0−13.4	7.0	7.2	23.0−29.4	26.8	27.3
4.	11°W − 20°W	30°N – 44°N	49760	0.2−19.6	8.0	7.6	13.3−20.4	16.4	16.3
5.	86°W −100°W	31°S – 60°S	200360	0.5−23.0	8.7	8.7	4.8−24.1	12.7	11.7
6.	171°W −180°W	15°S−14°N	123328	0.6−15.6	8.2	8.2	26.2−30.4	28.4	28.2
7.	31°W − 50°W	10°N – 29°N	90640	0.3−20.0	8.8	9.0	20.1−27.9	24.9	25.3
8.	140°W − 160°W	20°S − 30°S	50040	0.5−16.3	6.8	6.7	22.2−29.1	26.3	26.6
9.	140°W − 160°W	40°S − 50°S	41840	0.1−20.6	6.9	6.5	9.3−18.2	13.2	13.1
10.	0°W − 30°W	40°S − 50°S	133080	0.5−26.4	9.4	9.3	3.2−16.7	9.6	9.3
11.	50° E − 70° E	40°S − 50°S	50784	0.5−21.6	9.6	9.6	3.2−17.4	9.6	9.5
12.	180° E − 180°W	60°S − 90°S	576576	0.2−20.9	7.0	6.7	-1.9−8.0	1.8	1.4

* For January 2006.

b

Region	Lon.	Lat.	Number of samples**	Wind speed** [m s^{-1}]			SST**[˚C]		
				Range	Mean	Median	Range	Mean	Median
1.	86°W − 95°W	23°N–28°N	13848	0.4−10.0	4.5	4.4	28.7−30.5	29.5	29.4
2.	1°W − 15°W	1°S – 30°S	189600	0.2−14.0	6.6	6.6	17.7−27.1	23.2	23.7
3.	75° E − 89° E	1°S −30°S	195424	0.6−15.4	8.0	8.1	18.8−30.0	25.4	25.9
4.	11°W − 20°W	30°N – 44°N	43040	0.7−14.0	6.7	6.6	16.9−23.3	20.4	20.5
5.	86°W −100°W	31°S – 60°S	257496	0.7−22.7	9.8	9.6	2.5−19.1	9.3	8.3
6.	171°W −180°W	15°S−14°N	133096	0.1−14.8	6.0	6.0	26.9−29.7	28.8	29.0
7.	31°W − 50°W	10°N – 29°N	88304	0.4−13.6	7.4	7.4	23.6−28.0	26.0	26.1
8.	140°W − 160°W	20°S − 30°S	47504	0.7−24.7	6.9	6.2	18.8−27.0	23.2	23.4
9.	140°W − 160°W	40°S − 50°S	52736	0.5−21.0	10.1	10.3	8.2−14.1	10.9	10.8
10.	0°W − 30°W	40°S − 50°S	160192	0.9−28.9	10.8	10.8	1.8−14.6	8.3	8.3
11.	50° E − 70° E	40°S − 50°S	49344	1.1−28.2	12.9	12.7	2.1−16.1	8.3	7.8
12.	180° E − 180°W	60°S − 90°S	177240	0.8−29.1	11.7	11.9	-1.3−4.3	1.7	1.7

** For July 2006

Table 2

Regression coefficients n, a, and b with standard deviations σ derived as free parameters from fitting of Eq. (6) to different global data sets.

Data set	$n \pm \sigma_n$	$a \pm \sigma_a$	$b \pm \sigma_b$
W_{10}	$2.22 \pm 2.5\times10^{-4}$	$5.23\times10^{-5} \pm 4.5\times10^{-8}$	$-0.226 \pm 1.2\times10^{-3}$
W_{37}	$1.46 \pm 4.6\times10^{-4}$	$6.17\times10^{-4} \pm 9.1\times10^{-7}$	$-0.957 \pm 2.7\times10^{-3}$
W_{10} & W_{37}	$1.79 \pm 8.8\times10^{-4}$	$2.03\times10^{-4} \pm 5.9\times10^{-7}$	$-0.409 \pm 4.7\times10^{-3}$

Table 3

Results for slope (coefficient *m*) and intercept (coefficient *c*) from Eq. (8b) applied to satellite-based *W* data for March 2006 for all 12 regions for a) 10 GHz data; b) 37 GHz data. Mean wind speed U_{10} and sea surface temperature (SST) *T* for each region are also given. Such data were obtained for all months.

a) 10 GHz

region	slope	intercept	R^2	U_{10} (mean)	SST(mean)	No. data points
1	0.0098	-0.0077	0.9949	7.4003	23.7026	21304
2	0.0100	-0.0093	0.9920	6.4667	26.4579	208560
3	0.0101	-0.0097	0.9960	6.8460	27.1032	211152
4	0.0103	-0.0108	0.9960	8.2231	15.3210	64480
5	0.0103	-0.0116	0.9947	9.7639	13.2571	268320
6	0.0100	-0.0095	0.9958	6.0741	28.1153	140064
7	0.0101	-0.0094	0.9951	6.9834	23.9363	105848
8	0.0101	-0.0093	0.9932	6.3869	27.5344	58112
9	0.0101	-0.0106	0.9938	8.0021	13.8762	52952
10	0.0102	-0.0109	0.9953	8.7709	10.5947	161776
11	0.0103	-0.0115	0.9928	9.2368	11.5374	55200
12	0.0103	-0.0115	0.9944	9.2582	1.8162	1039264

b) 37 GHz

region	slope	intercept	R^2	U_{10} (mean)	SST(mean)	No. data points
1	0.0100	0.0227	0.9574	7.3949	23.7273	18056
2	0.0109	0.0139	0.9453	6.4370	26.4630	191728
3	0.0103	0.0154	0.9518	6.6755	27.1823	185224
4	0.0099	0.0262	0.9604	8.2645	15.3113	55216
5	0.0100	0.0241	0.9589	9.7181	13.3633	242792
6	0.0098	0.0165	0.9381	5.9357	28.0589	125632
7	0.0107	0.0189	0.9784	6.8255	23.8623	96440
8	0.0098	0.0180	0.9657	6.2512	27.5191	54712
9	0.0101	0.0212	0.9447	8.0332	13.9375	48888
10	0.0099	0.0247	0.9521	8.4807	10.6534	150920
11	0.0098	0.0261	0.9165	9.0372	11.6882	51784
12	0.0096	0.0278	0.9338	9.0238	1.8538	922080

Table 4

Coefficients for the SST dependence of the parametric coefficients a and b in Eq. (14). The temperature dependent parametric coefficients $a(T)$ and $b(T)$ are used in parameterization $W(U_{10}, T)$ (Eq. (13)) derived from satellite-based W data for 10 and 37 GHz for 2006.

Data set	a_0	a_1	a_2	b_0	b_1
W_{10}	1.08×10^{-4}	-2.45×10^{-7}	-1.45×10^{-9}	-1.203	9.9612×10^{-3}
W_{37}	8.46×10^{-5}	1.63×10^{-6}	-3.35×10^{-8}	3.354	-6.2×10^{-2}

Figure captions

Figure 1. Satellite retrieved 37 GHz W data for 11 March 2006. a) Map (0.5°×0.5°) of ascending and descending passes for W at 37 GHz; b) W at 10 and 37 GHz (green and magenta symbols, respectively) compared to historical photographic data including total W (diamonds) and active whitecap fraction W_A (squares). Parameterization $W(U_{10})$ of Monahan and O'Muircheartaigh (1980, MOM80) (purple line) is shown for reference.

Figure 2. Selected regions to determine regional variations of $W(U_{10})$.

Figure 3. Seasonal cycle for 2006 in different regions as defined in Fig. 2 and Table 1: a) wind speed U_{10}; b) Sea surface temperature (SST) T. The regions represent: 4–Temperate zone in Northern hemisphere; 5–Temperate zone in Southern hemisphere; 6–Doldrums along the Equator; 12–Lowest SST.

Figure 4. Scatter plot for March 2006 of (a) global $U_{10ECMWF}$ versus $U_{10QSCAT}$ and (b) global T from ECMWF versus T from GDAS. In both figures the colors indicate the amount of data points per hexabin. The black lines are linear fits: the dashed line represents unrestricted fit and the solid line a fit forced through zero. The linear regressions and respective R^2 are listed in each panel.

Figure 5. Global W as function of U_{10} from QuikSCAT for March 2006 where W is obtained with 10 GHz (a) and 37 GHz (b) measurement frequency. Panels c and d plot the data in panels a and b with logarithmic y-axis. The red line indicates the Monahan and O'Muircheartaigh (1980, MOM80) relationship (Eq. (3)). The colors indicate the amount of data points per hexabin.

Figure 6. Global $W^{1/2}$ as function of U_{10} from QuikSCAT for March 2006, where $W^{1/2}$ is obtained with 10 GHz (a) and 37 GHz (b) measurement frequency. The black line in both panels indicates the best linear fit through the data. The red line in Fig. 6b equals the black line in Fig. 6a. The colors indicate the amount of data points per hexabin.

Figure 7. Scatter plots of W data for 37 GHz versus $U_{10ECMWF}$ for March 2006: a) $W^{1/2}$; b) W obtained with Eq. (12). The black lines in panel a are linear fits: the dashed line represents unrestricted fit and the solid line is a fit forced through zero. The linear fits and respective R^2 are listed. The red line in panel b indicates the Monahan and O'Muircheartaigh (1980, MOM80) relationship (Eq. (3)). The colors indicate the amount of data points per hexabin.

Figure 8: Scatter plots of residuals ΔW between W data for 37 GHz from the whitecap database and parameterized W values as a function of wind speed from different sources: a) Wind speed values $U_{10QSCAT}$ from the whitecap database used with Eq. (11); b) Wind speed values $U_{10ECMWF}$ from the ECMWF model used with Eq. (12). The rms deviations for each data set is given in each panel.

Figure 9. Linear fits of $W^{1/2}$ versus U_{10} for: region 1 for January 2006 at 10 GHz (a) and 37 GHz (b); region 5 for all months at 10 GHz (c) and 37 GHz (d); regions 1-12 for March 2006 at 10 GHz (e) and 37 GHz (f).

Figure 10. Regional and seasonal variations: a) Regionally averaged b values for each month with error bars (± one standard deviation) representing the regional variability; b) Annually averaged b values for each region with error bars representing the seasonal variability.

Figure 11. Sea surface temperature dependences of a) coefficient a (slope) and b) coefficient b (intercept) in the $W(U_{10})$ dependence. Each point is annual mean for different region. The error bars indicate ± 1 standard deviation for SST (horizontal bars) and coefficients (vertical bars). Panel c) shows the monthly means of coefficients b for each region that form one data point in panel b). Regions in Northern hemisphere (NH) are show with squares; regions in Southern hemisphere (SH) are shown with circles. The diamonds are for region 6 at the Equator.

Figure 12. a) Comparison of the new parameterization $W(U_{10}, T)$ (Eqs. 13-14) at three fixed SST values (T = 20 °C, red line; T = 12 °C, green line; T = 2 °C, blue line) to the global parameterization $W(U_{10})$ (Eq. 11, black solid line) and the parameterizations of Salisbury et al. (2013, SAL13) (Eq. (1)) for 37 GHz (magenta line) and Monahan and O'Muircheartaigh (1980, MOM80) (Eq. (3)) (purple line).

c) Comparison of the new $W(U_{10}, T)$ parameterizations with quadratic (Eqs. 13-14, blue line) and cubic (green line) wind speed exponents at T = 20 °C to the parameterizations of Salisbury et al. (2013, SAL13) (Eq. (1)) for 37 GHz (magenta line) and Monahan and O'Muircheartaigh (1980, MOM80) (purple line).

Figure 13. a) In situ W data as in Fig. 1b (gray symbols) and satellite-based W data for 17 March 2007 at 10 and 37 GHz (green and magenta symbols, respectively) compared to W values obtained from $W(U_{10})$ for 10 and 37 GHz (black lines, Eqs. (10-11)) and $W(U_{10}, T)$ for

Deleted: 8

Deleted: $\sqrt{W}$

Deleted: Figure 9. Seasonal cycle for 2006 of regression coefficients in the $\sqrt{W}(U_{10})$ linear fits for different regions as defined in Fig. 2 and Table 1: a) slope m; b) y-intercept c.. The regions represent: 4–Temperate zone in Northern hemisphere; 5–Temperate zone in Southern hemisphere; 6–Doldrums along the Equator; 12–Lowest SST. ¶

Deleted: Comparison of the new global $W(U_{10})$ parameterization (based on the global W data set) to parameterizations from different studies: SAL13 (10 GHz) and SAL13 (37 GHz) are parameterizations from Salisbury et al. (2013) (Eq. (1)), CAL08 are parameterizations derived by Callaghan et al. (2008) (Eq. (2)); and MOM80 is the parameterization of Monahan and O'Muircheartaigh (1980) (Eq. (3)).¶ b)

Deleted: quadratic

Deleted: quadratic

Deleted: 10 GHz (dash-dotted line) and

Deleted: dashed

Deleted: .

Deleted: purple

Deleted: red

Deleted: dashed

Deleted: blue solid

Deleted: A

Deleted: with

Deleted: added

10 (red) and 37 GHz (cyan, Eqs. (13-14)). Wind speed and sea surface temperature from the whitecap database are used for the calculations.

b) Difference map of annual average W distribution for 2006 calculated from the Monahan and O'Muircheartaigh (1980, MOM80) $W(U_{10})$ parameterization (Eq. (3)) minus $W(U_{10}, T)$ from Eqs. (13-14) The calculations use wind speed U_{10} is from QuikSCAT in the whitecap database.

Figure 14. a) Annual average super-micron mass emission rate for 2006 in μg m^{-2} s^{-1} calculated from from Eq. (4′)). b) Difference map between the annual average super-micron SSA mass emission rate calculated from the Monahan et al. (1986) SSSF and the annual average super-micron SSA mass emission rate calculated from the Monahan et al. (1986) SSSF where W is replaced with Eqs. (13-14). The calculations use wind speed U_{10} is e from QuikSCAT in the whitecap database.

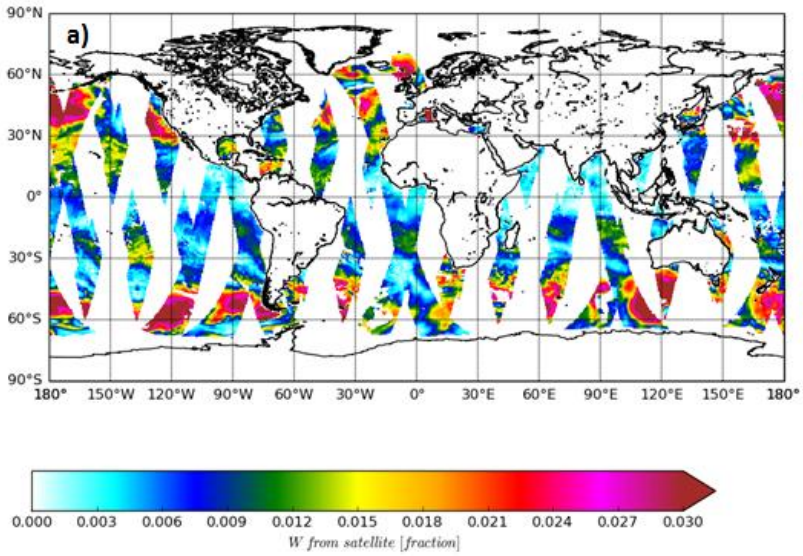

1

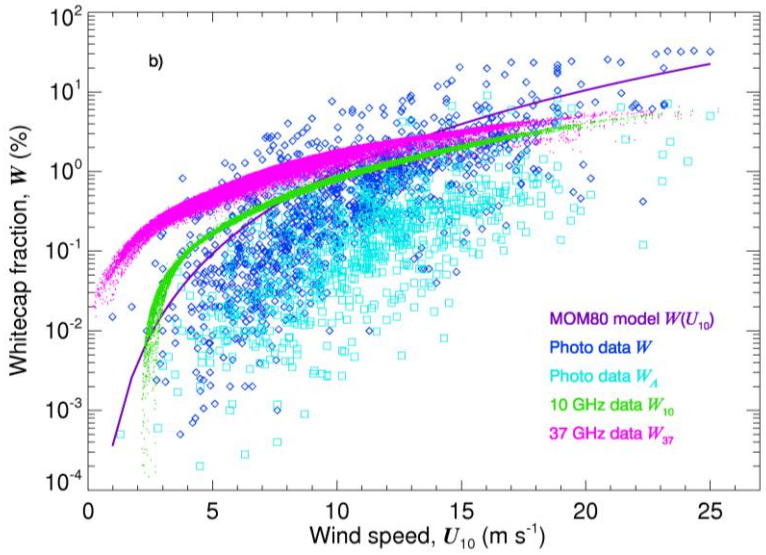

2

3 Figure 1

4

1

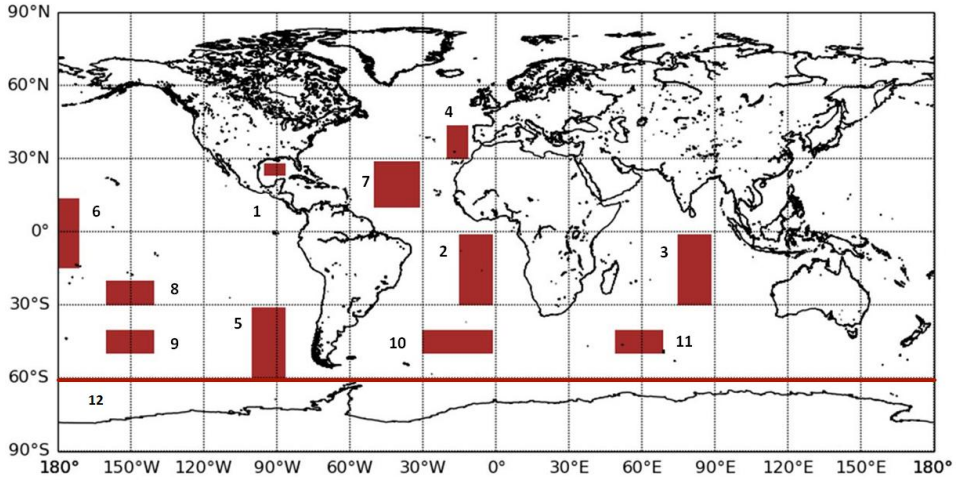
90°N
60°N
30°N
0°
30°S
60°S
90°S
180°
150°W
120°W
90°W
60°W
30°W
0°
30°E
60°E
90°E
120°E
150°E
180°
1
2
3
4
5
6
7
8
9
10
11
12

Figure 2

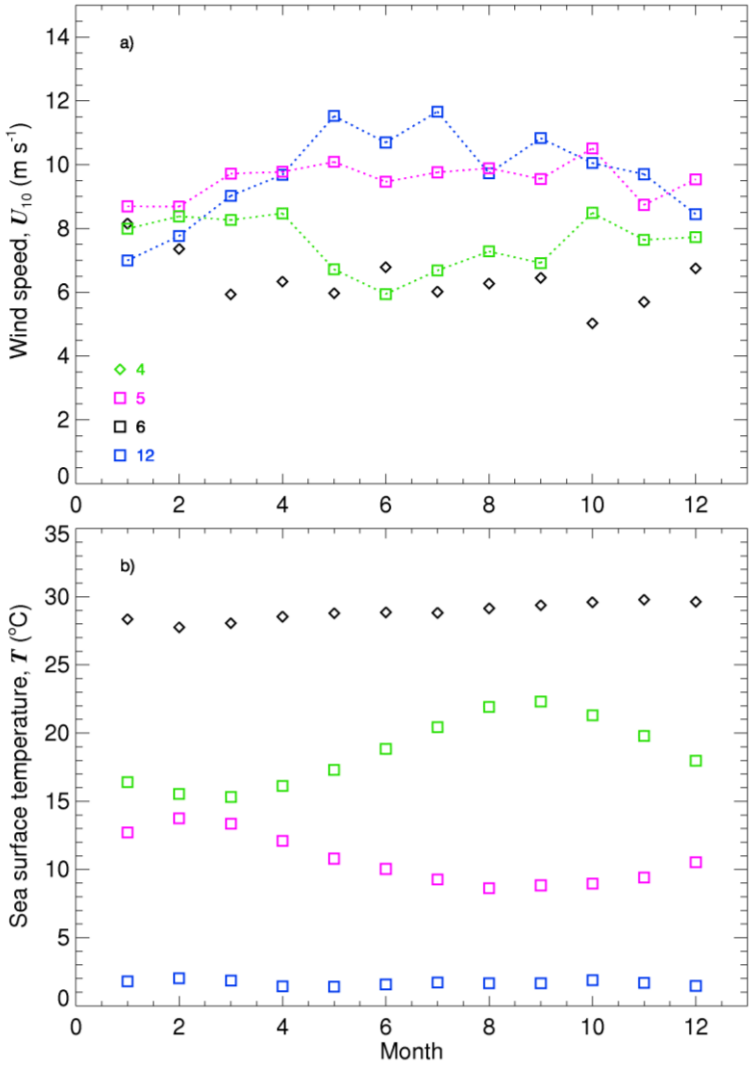
a)
Wind speed, U_{10} (m s^{-1})
4
5
6
12
b)
Sea surface temperature, T (°C)
Month

Figure 3

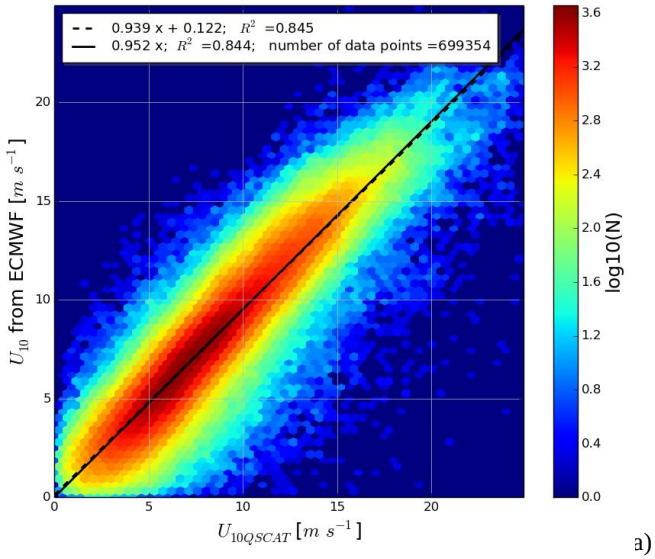
0.939 x + 0.122; R^2 =0.845
0.952 x; R^2 =0.844; number of data points =699354
U_{10} from ECMWF [$m\ s^{-1}$]
$U_{10QSCAT}$ [$m\ s^{-1}$]
log10(N)

a)

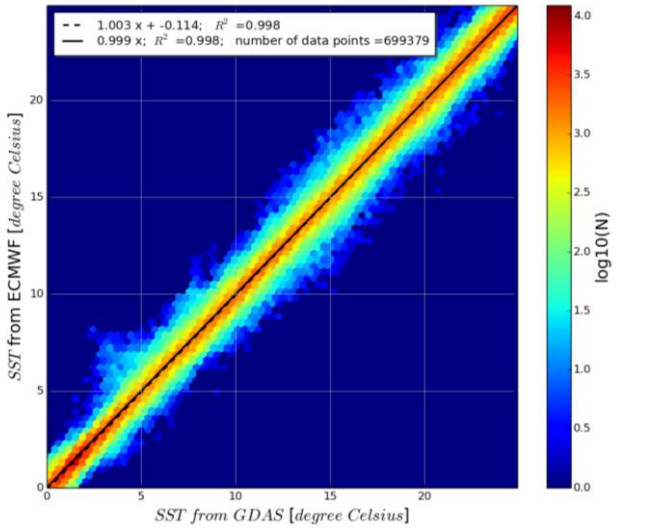
1.003 x + -0.114; R^2 =0.998
0.999 x; R^2 =0.998; number of data points =699379
SST from ECMWF [degree Celsius]
SST from GDAS [degree Celsius]
log10(N)

b)

Figure 4

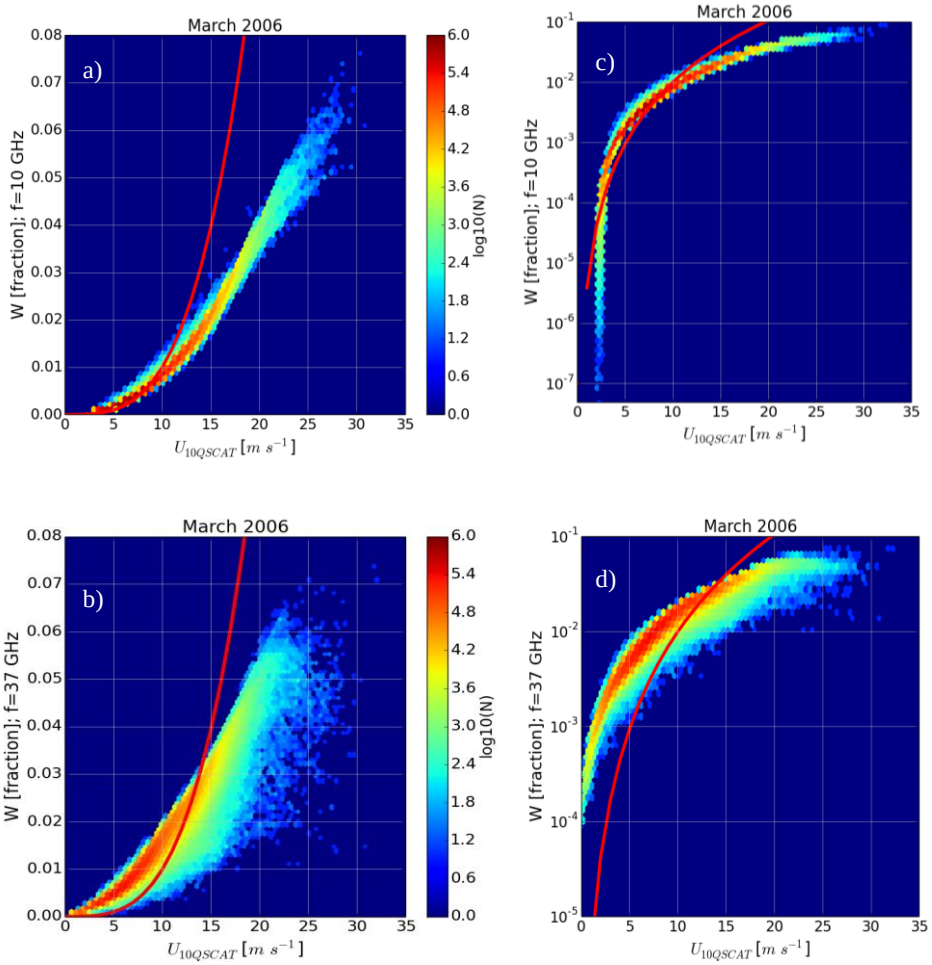

a

b

Figure 5

Deleted:

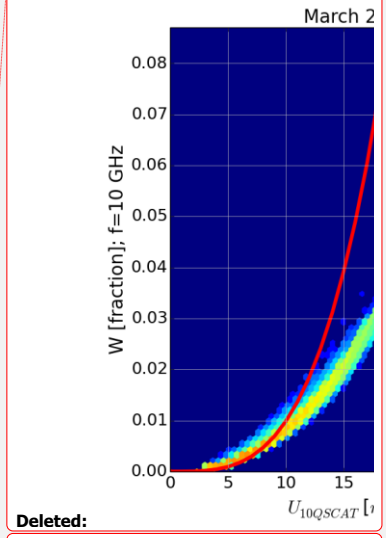

Deleted:

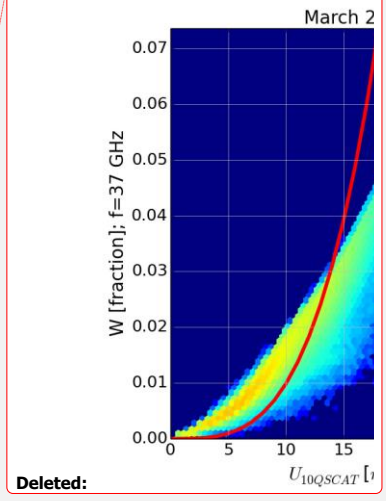

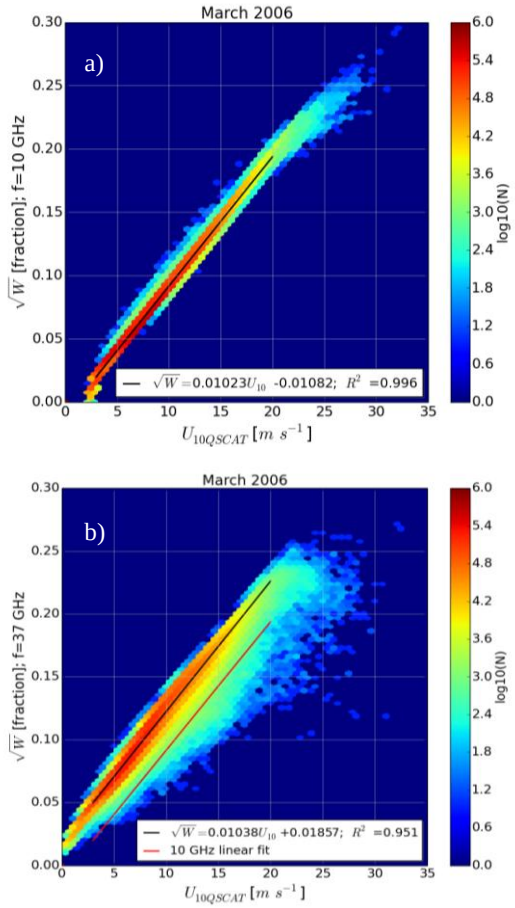

Figure 6

Deleted: a

Deleted: b

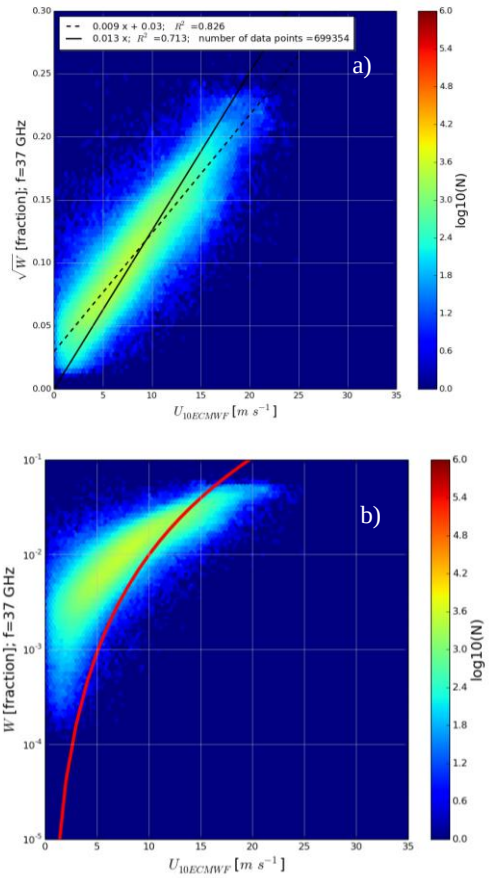

Figure 7

Deleted: a

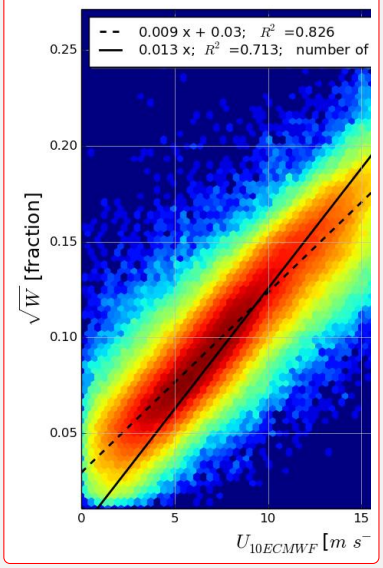

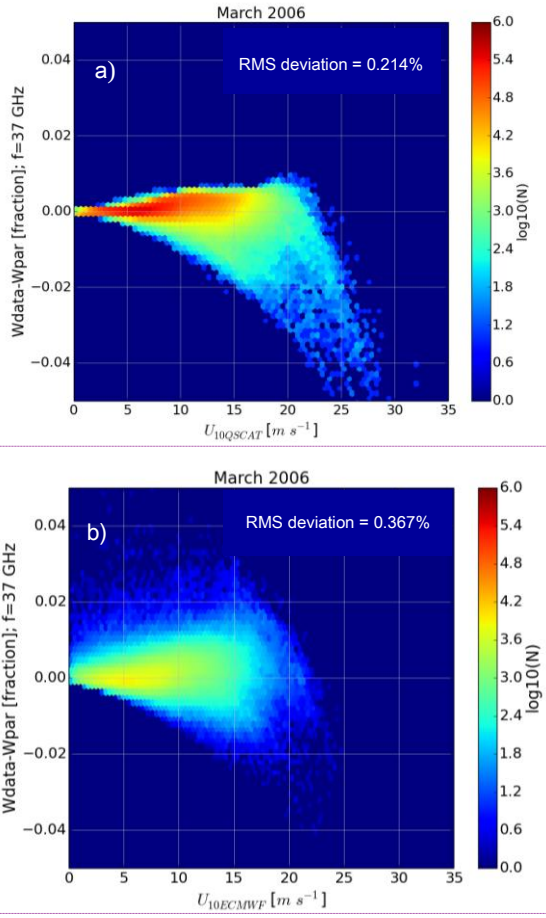

Figure 8

Formatted: Font color: Auto

Formatted: Font color: Auto

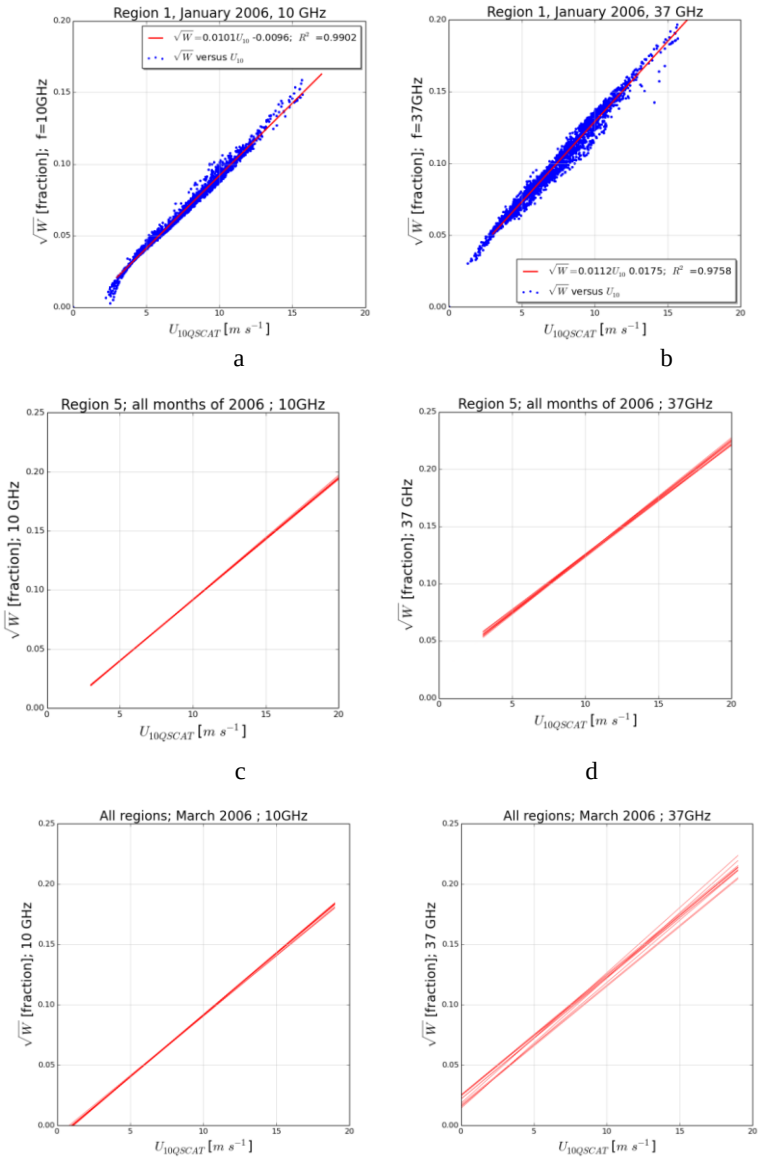

Figure 9

Formatted: Justified

Deleted: 8

Deleted: ¶

¶

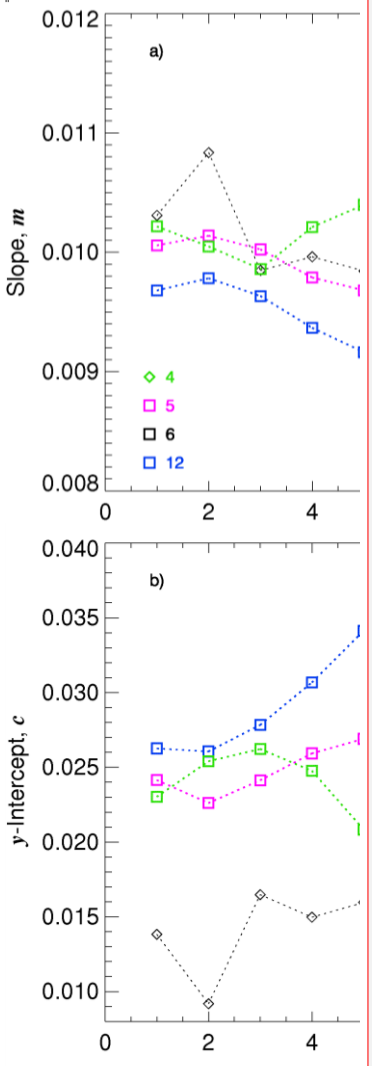

Figure 9 ¶

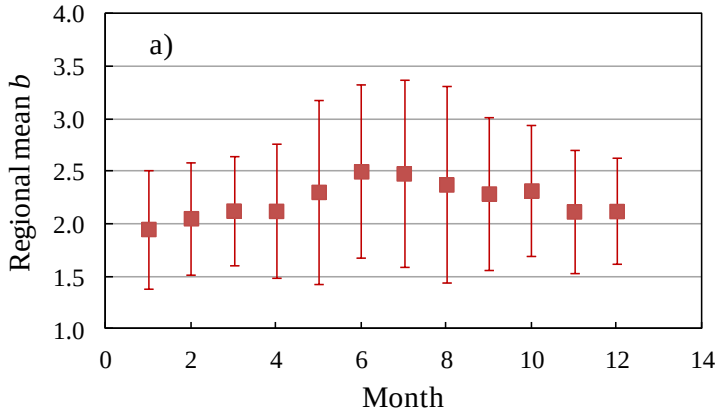
a)
Regional mean b
4.0
3.5
3.0
2.5
2.0
1.5
1.0
0
2
4
6
8
10
12
14
Month

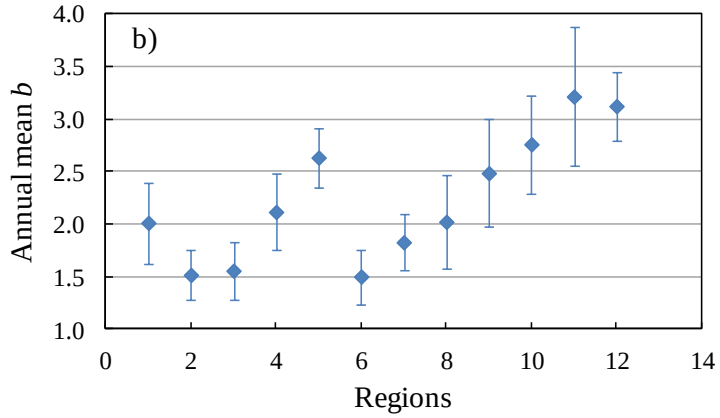
b)
Annual mean b
4.0
3.5
3.0
2.5
2.0
1.5
1.0
0
2
4
6
8
10
12
14
Regions

Figure 10

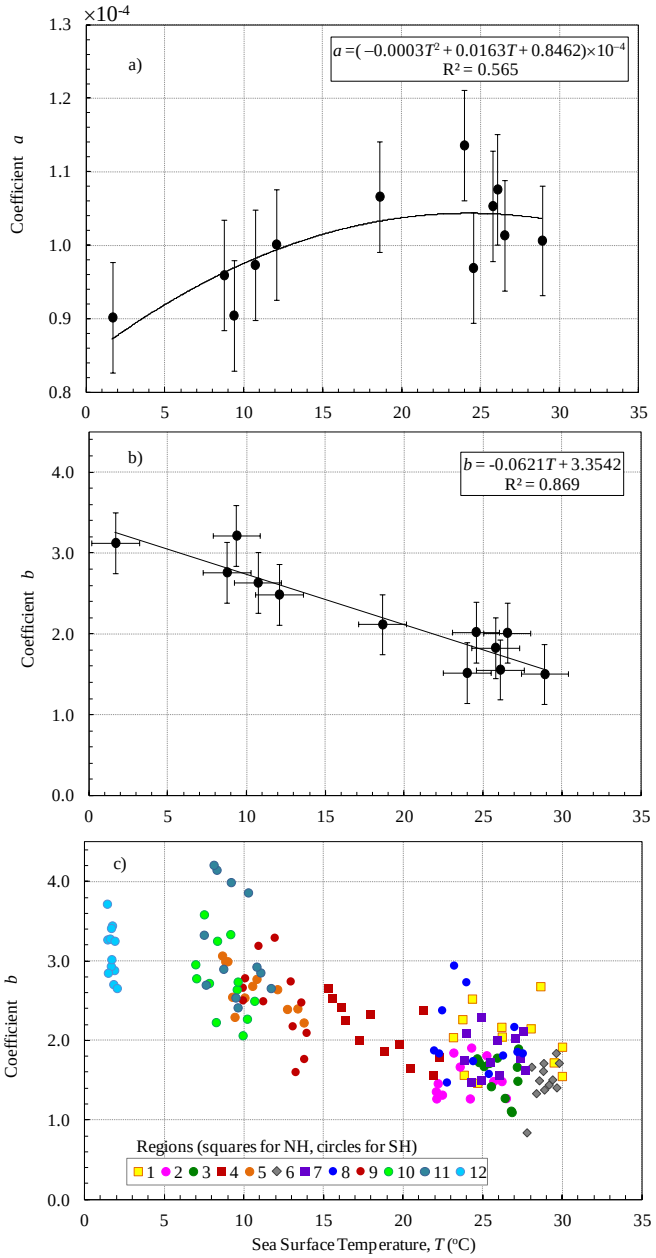
×10-4
a)
a =(–0.0003T² + 0.0163T + 0.8462)×10-4
R² = 0.565
Coefficient a
b)
b = -0.0621T + 3.3542
R² = 0.869
Coefficient b
c)
Coefficient b
Regions (squares for NH, circles for SH)
1 2 3 4 5 6 7 8 9 10 11 12
Sea Surface Temperature, T (ºC)

Figure 11

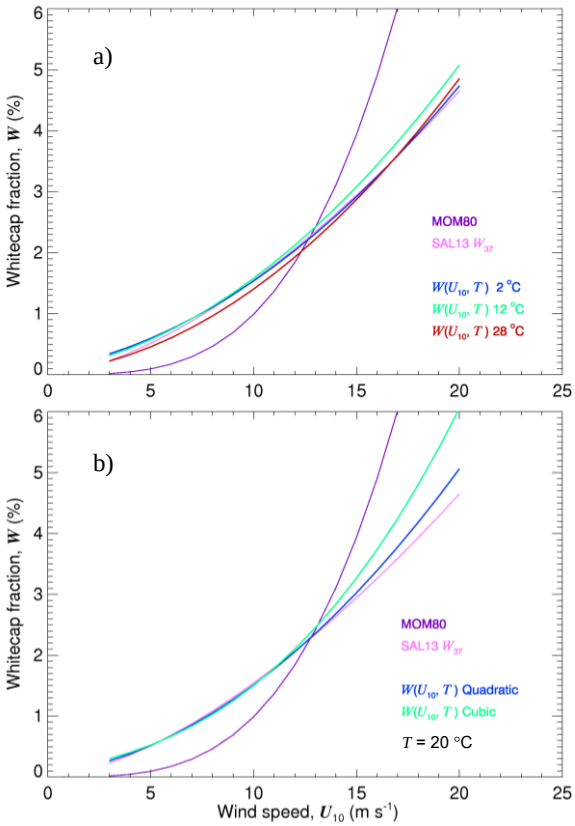

Figure 12

Deleted:

a)
Whitecap fraction, W (%)

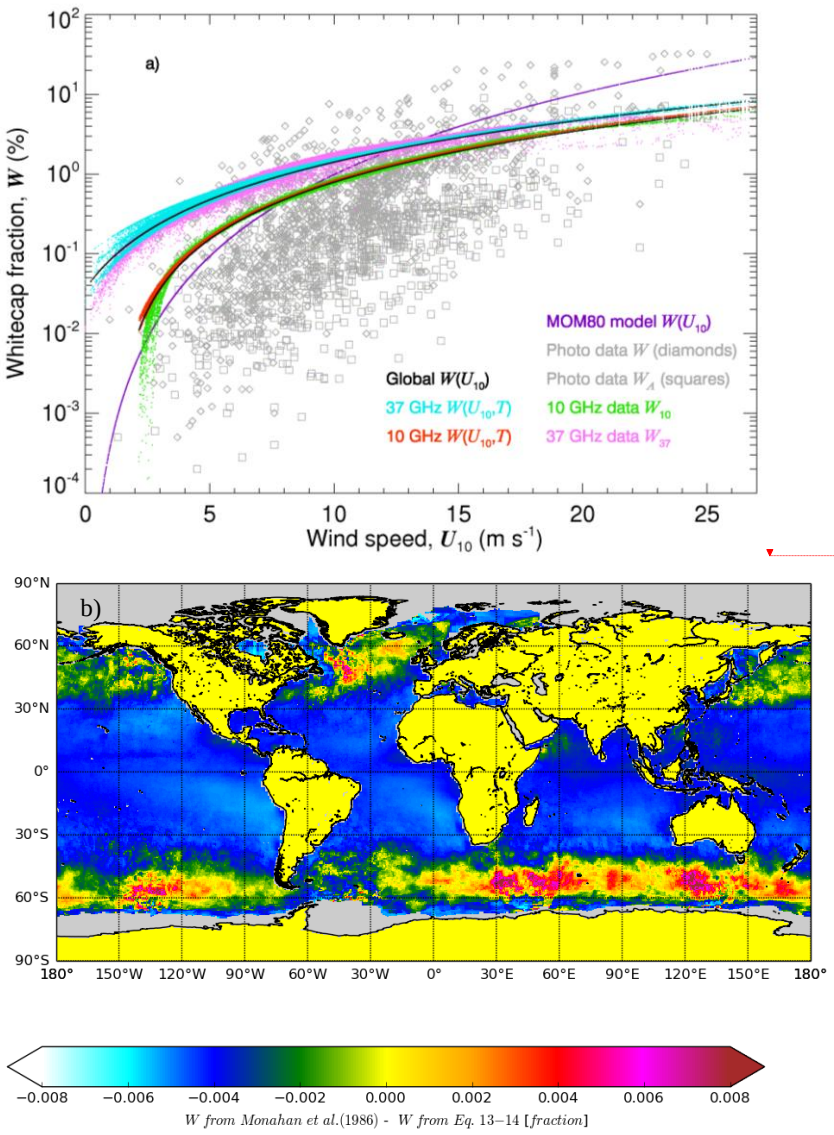

Deleted:

Figure 13

1

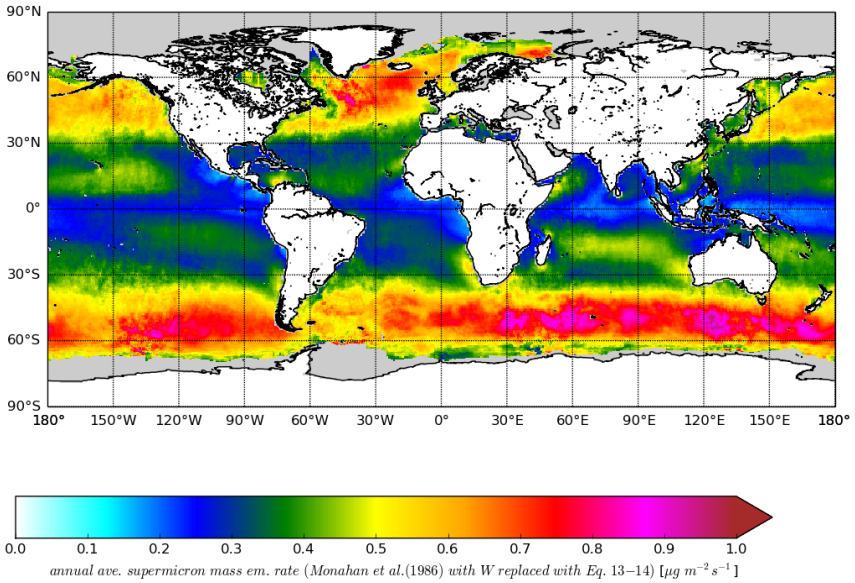

2

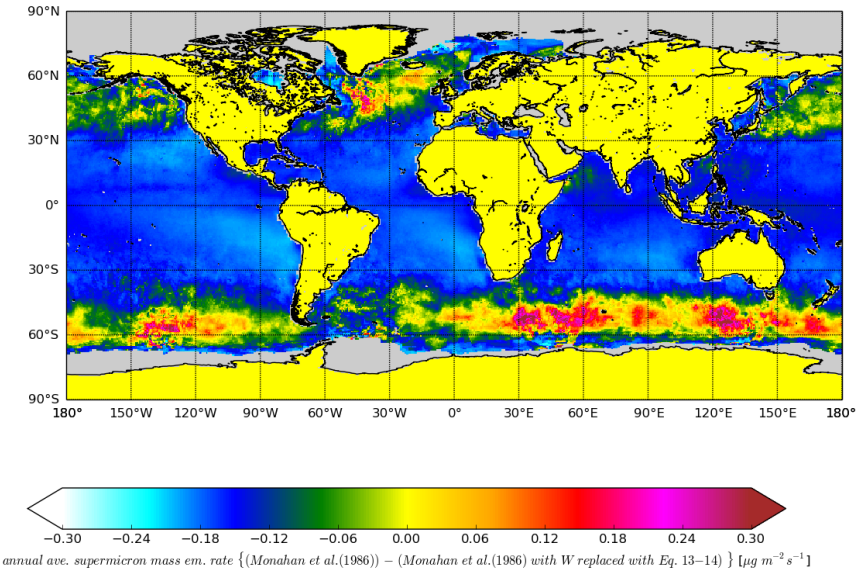

3

4 Figure 14